

Structure-based control of complex networks with nonlinear dynamics

Jorge G. T. Zañudo,^{1,*} Gang Yang,¹ and Réka Albert^{1,2}

¹*Department of Physics, The Pennsylvania State University,
University Park, Pennsylvania, 16802-6300, USA.*

²*Department of Biology, The Pennsylvania State University,
University Park, Pennsylvania, 16802-5301, USA.*

What can we learn about controlling a system solely from its underlying network structure? Here we use a framework for control of networks governed by a broad class of nonlinear dynamics that includes the major dynamic models of biological, technological, and social processes. This feedback-based framework provides realizable node overrides that steer a system towards any of its natural long term dynamic behaviors, regardless of the dynamic details and system parameters. We use this framework on several real networks, compare its predictions to those of classical structural control theory, and identify the topological characteristics that underlie the observed differences. Finally, we demonstrate this framework's applicability in dynamic models of gene regulatory networks and identify nodes whose override is necessary for control in the general case, but not in specific model instances.

Controlling the internal state of complex systems is of fundamental interest and enables applications in biological, technological and social contexts. An informative abstraction of these systems is to represent the system's elements as nodes and their interactions as edges of a network. Often asked questions related to control of a networked system are how difficult to control it is, and which network elements play an important role in controlling it [1–7]. Control theory provides well developed mathematical frameworks that allow a variety of control-related questions to be addressed [8, 9]. Structural controllability (SC), introduced by Lin, distinguishes itself among these methods due to its ability to draw strong dynamical conclusions based solely on network structure and unspecified linear time-invariant dynamics [10, 11].

Despite its success and wide-spread application [4, 12–18], SC may give an approximate answer to the question of how difficult to control a system is. It can only provide sufficient conditions to control systems with nonlinear dynamics [1, 18], and its definition of control (full control; from any initial to any final state) does not always match the meaning of control in biological, technological, and social systems, in which control tends to involve only naturally occurring system states [19]. Several new methods of control have been proposed to incorporate the inherent nonlinear dynamics of real systems and relax the definition of full control [5, 7, 18, 20, 21]. Only one of these methods, namely feedback vertex set control (FC), can be reliably applied to large complex networks in which only the structure is well known. This method, based on the mathematical framework in [3, 22], incorporates the nonlinearity of the dynamics and considers only the naturally occurring end states of the system as desirable final states. In this work, we study whether a complex network is difficult to control using SC and FC as benchmark methods, and identify the topological characteristics that underlie their commonalities and differences.

I. THE ROLE OF DYNAMICS IN STRUCTURE-BASED NETWORK CONTROL

Most real systems are driven by nonlinear dynamics in which a decay term prevents the system's variables from increasing without bounds. The state of the system's N nodes at time t , characterized by source node variables $S_j(t)$ (for nodes with no incoming edges) and internal node variables $X_i(t)$, obeys the equations

$$\frac{dX_i}{dt} = F_i(X_i, X_{I_i}, t), \quad i = 1, 2, \dots, N - N_s, \quad (1)$$

$$S_j(t) = E_j(t), \quad j = N - N_s + 1, \dots, N, \quad (2)$$

where N_s is the number of source nodes. The dynamics of each source node j is determined by an environmental signal $E_j(t)$, while the dynamics of each internal node i is governed by $F_i(X_i, X_{I_i}, t)$, which captures the nonlinear response of node i to its predecessor nodes I_i , and which includes decay in the dependence of F_i on X_i (Supplementary Text). Functions of the form $F_i = f_i(X_{I_i}) - \alpha_i(X_{I_i})X_i$, which satisfy these conditions, are used to describe the dynamics of birth-death processes [23], epidemic processes [25], biochemical dynamics [26, 27], and gene regulation [26, 27]. In many systems there is adequate knowledge of the underlying wiring diagram but not of the specific parameter values required to fully specify F_i and E_j . Analyzing such systems requires the use of structure-based control methods such as structural controllability and feedback vertex set control.

In structural controllability (SC) the objective is to drive the system from any initial state to any final state in finite time (i.e. full control, Fig. 1a) by manipulating the state of the system using a certain number of external driver node signals $\mathbf{u}(t) = (u_1(t), \dots, u_M(t))$. The dynamics of the system are considered to be well approximated by linear dynamics (e.g., by linearizing Eq.

* Corresponding author: jgtz@phys.psu.edu

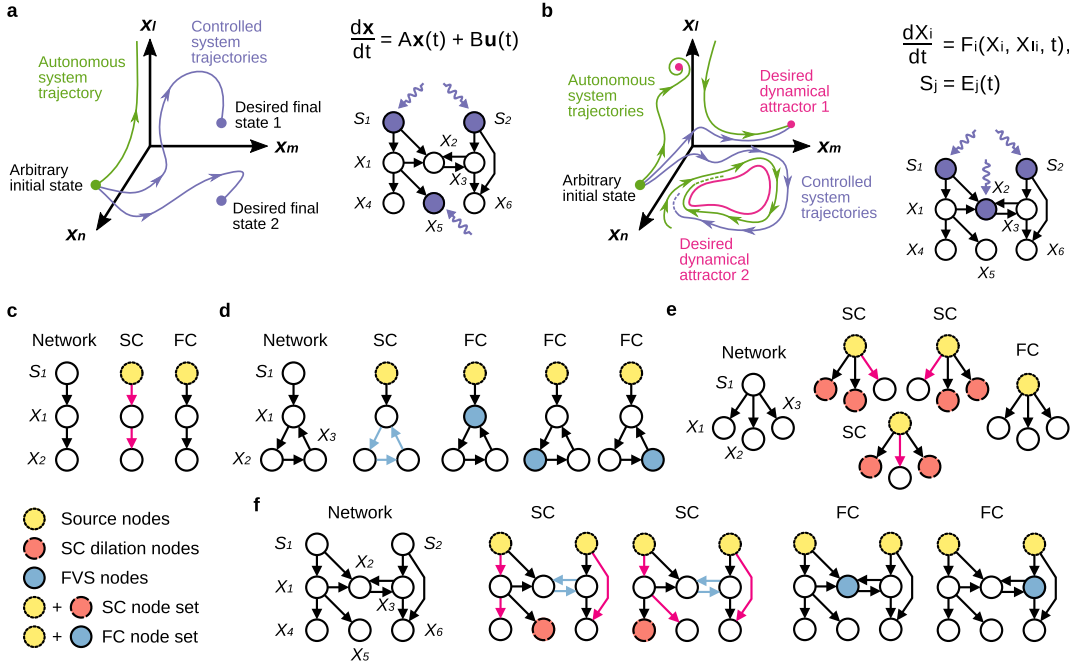


Fig. 1. Structure-based control methods. Structure-based control methods make strong conclusions about the dynamics of a system using solely the network structure. (a) In structural controllability (SC) the objective is to drive the network from an arbitrary initial state to any desired final state by acting on the network with an external signal $\mathbf{u}(t)$. The dynamics are considered to be well-approximated by linear dynamics. (b) In feedback vertex set control (FC) the objective is to drive the network from an arbitrary initial state to any desired dynamical attractor (e.g. fixed point) by overriding the state of certain nodes. (c-f) Structure-based control in simple networks. Control of the source nodes (yellow nodes with dotted outlines) is shared by SC and FC. SC additionally requires controlling certain dilation nodes (red nodes with dashed outlines) but requires no independent control of cycles. FC requires controlling all cycles by control of the feedback vertex set (FVS, blue nodes with solid outlines). The edges of the non-intersecting linear chains of nodes of SC are colored purple and the edges involved in a directed cycle are colored blue.

1 around a state of interest, see Supplementary Text)

$$\frac{d\mathbf{x}}{dt} = A\mathbf{x}(t) + B\mathbf{u}(t), \quad (3)$$

where $\mathbf{x}(t)$ is a vector composed of all the X_i 's and S_j 's, A is a $N \times N$ matrix that encodes the wiring diagram of the network and is such that a_{ik} is nonzero only if node i is a successor of node k (i.e., there is a directed edge from k to i), and B is a $N \times M$ matrix that describes which nodes X_i and E_j are driven by the external signals $\mathbf{u}(t)$. This system is such that if it can be controlled in the specified way by a given pair (A, B) , this will also be true for almost all pairs (A, B) (except for a set of measure zero) [8, 10, 11]. In other words, SC is necessary and sufficient for full control of a system governed by Eq. 3 for almost all A 's consistent with the network wiring diagram.

SC is a mathematical formalization of the idea that a node can fully manipulate only one of its successor elements at a time and that a directed cycle is inherently self-regulatory. A consequence of this is that the driver nodes are such that every network node is either part of a set of non-intersecting linear chains of nodes that begin at the driver nodes or is part of a set of directed cycle that do not intersect each other or the set of linear chains (Fig. 1). As Ruths & Ruths showed [6], this

implies that there are three types of network nodes that must be directly manipulated by a unique driver node, and which we call SC nodes: (i) every source node, and every successor node of a dilation (when a node has more than one successor node) that is not part of the set of linear chains or of the cycles, namely (ii) the surplus of sink nodes with respect to source nodes or (iii) internal dilation nodes.

An alternative structure-based control method for networks that lack source nodes was developed by Fiedler, Mochizuki et al. [3, 22]. This method is a mathematical formalization of the following idea: in order to drive the state of a source-less network to any one of its dynamical attractors one needs to manipulate a set of nodes that intersects every feedback loop in the network - the feedback vertex set (FVS). This requirement encodes the importance of feedback loops in determining the dynamical attractors of the network, a fact that was recognized early on in the study of the dynamics of biological networks [28, 29]. Fiedler, Mochizuki et al. mathematically proved that for a network governed by the nonlinear dynamics in Eq. 1, locking the feedback vertex set of the network in the trajectory specified by a given dynamical attractor ensures that the network will asymptotically approach the desired dynamical attractor, regardless of the specific form of the functions F_i . Controlling the

FVS is both necessary and sufficient to drive the system to the desired attractor for every form of F_i ([3, 22] and Supplementary Text).

Here we extend this structural theory to networks in which source nodes are governed by Eq. 2 (Fig. 1b and Supplementary Text). Since the source nodes are unaffected by other nodes, one additionally needs to lock the source nodes of the network in the trajectory specified by the attractor. In summary, control of the source nodes and of the feedback vertex set of a network guarantees that we can guide it from any initial state to any of its dynamical attractors (i.e., its natural long term dynamic behavior) regardless of the specific form of the functions F_i and E_j . In the following we refer to this attractor-based control method as feedback vertex set control (FC) (Fig. 1b), and to the group of nodes that need be manipulated in feedback vertex set control as a FC node set.

To illustrate structural controllability and feedback vertex set control, consider the example networks in Fig. 1. In a linear chain of nodes (Fig. 1c, left) the only node that needs to be controlled in both frameworks is the source node S_1 . For Fig. 1d, which consists of a source node connected to a cycle, SC requires controlling only the source node S_1 since the cycle is considered self-regulating (Fig 1d, middle), while FC additionally requires controlling any node X_i in the cycle, the feedback vertex set in this network (Fig. 1d, right). Fig 1e consists of a source node with three successor nodes; SC requires controlling two of the three successor nodes because of the dilation at the source node S_1 , while for FC controlling S_1 is sufficient. In Fig 1f we show a more complicated network with a cycle and several source and sink nodes, and two minimal node sets for SC and FC. These examples illustrate that the control of the source nodes is shared by full control in SC and attractor control in FC, and that their main difference is in the treatment of cycles, which require to be controlled in FC and do not require independent control in SC.

II. STRUCTURE-BASED CONTROL OF REAL NETWORKS

SC was applied to diverse types of real networks and the ratio of the minimal number of SC nodes needed, N_{SC} , and the total number of nodes, $n_{SC} = N_{SC}/N$ was used to gauge how difficult it is to control these networks [1]. Both SC and FC can be used to answer the question of how difficult to control a network is (albeit each focuses on a different aspect of control, full control or attractor control), so a natural question is how the fraction of control nodes in real networks compares between SC and FC ($n_{FC} = N_{FC}/N$, where N_{FC} is the size of the minimal FC control set). To answer this question, we apply SC and FC to the real networks in [1], and compare the fraction of control nodes n_{SC} and n_{FC} (Fig. 2a and Table S1). A surprising result is that the fraction

of control nodes n_{SC} and n_{FC} appears to be inversely related across several types of networks. For example, gene regulatory networks require between 75% - 96% of nodes in SC yet only require between 1% - 18% of nodes in FC. A similar $n_{SC} \gg n_{FC}$ relationship is also seen in food web networks and internet networks, while the opposite relationship ($n_{SC} \ll n_{FC}$) is seen in the social trust networks with low n_{SC} and intra-organizational networks. On further reflection, FC's prediction that gene regulatory networks are easier to control than social trust/communication networks is supported by recent experimental results in cellular reprogramming and large-scale social network experiments [19, 30].

To explain the topological properties underlying the difference in n_{SC} and n_{FC} , we note that the fraction of nodes n_{SC} and n_{FC} obey the relations

$$n_{SC} = n_s + n_e + n_i, \quad (4)$$

$$n_{FC} = n_s + n_{FVS}, \quad (5)$$

where n_s is the fraction of source nodes, n_e is the fraction of external dilations nodes in SC, n_i is the fraction of internal dilation nodes in SC, and n_{FVS} is the fraction of nodes in the FVS of the network. Empirical directed networks tend to have a bow-tie structure [31], in which most of the network belongs to the largest strongly connected component (which contains most cycles in the network, and thus determines n_{FVS}), its in-component (the nodes that can reach the strongly connected component, which thus determine n_s), or its out-component (the nodes that can be reached from the strongly connected component, which thus determine n_e). We define the fractions $\eta_x = n_x / (n_s + n_e + n_i + n_{FVS})$, where $x = s, e, i, FVS$. These fractions reflect the potential domination of a network component over the others. Eqs. 4-5 and the bow-tie structure of real networks offer a topological explanation for the observed relationships between n_{SC} and n_{FC} .

Applying this reasoning to the studied real networks (Table S1), we find that all networks with $n_{SC} < n_{FC}$ have a topology dominated by their SCC component ($\eta_{FVS} \gg \eta_e, \eta_i, \eta_s$, Fig. 2, brown shading; e.g. intra-organizational networks, the college students and prison inmates trust networks, and the *C. elegans* neural network). Most networks with $n_{SC} > n_{FC}$ are dominated by their out-component ($\eta_e \gg \eta_{FVS}, \eta_i, \eta_s$, Fig. 2, yellow shading; e.g. gene regulatory networks, most food webs, and internet networks) or by internal dilations ($\eta_i \gg \eta_{FVS}, \eta_e, \eta_s$, Fig. 2, pink shading; e.g. metabolic networks and circuits). The rest of the networks have a mixed profile ($\eta_{FVS} \simeq \eta_e \simeq \eta_i \simeq \eta_s$, Fig. 2, no shading), and include networks with $n_{SC} > n_{FC}$ (citation networks and the Texas power grid) and the networks in which $n_{SC} \simeq n_{FC}$ (a political blog network and two online social communication networks).

Motivated by the observed remarkable agreement between the number of SC nodes n_{SC} of real networks and their degree-preserving randomized versions [32], we study FC control in similarly randomized real networks

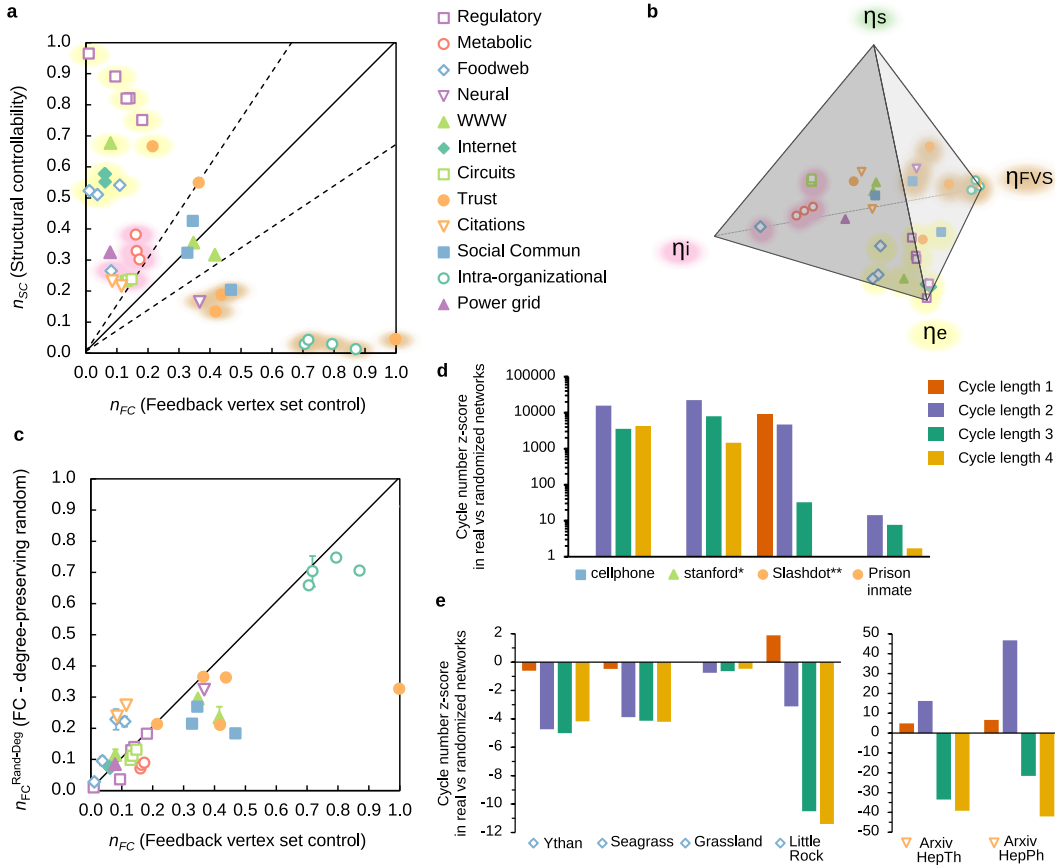


Fig. 2. Structure-based control in real networks. (a) Scatter plot with the fraction of control nodes in feedback vertex set (FVS) control (n_{FC}) and structural controllability (n_{SC}) for each real network in Table S1. The bold line denotes the positions in the plot with $n_{SC} = n_{FC}$, while the dashed lines denote $n_{SC} = 1.5 n_{FC}$ and $n_{FC} = 1.5 n_{SC}$. The shading of the symbols corresponds to their position in panel b. (b) Barycentric plot of the normalized fraction of control nodes η_x , where $x = s, e, i, FVS$ for each real network. The position in the plot is determined by η_x in such a way that a point is close to the η_x vertex if $\eta_x \simeq 1$ and close to the face opposite to the η_x vertex if $\eta_x \simeq 0$. Thus, networks dominated by their FVS and strongly connected component are close to the η_{FVS} vertex (brown shading), networks dominated by their out-component are close to the η_e vertex (yellow shading), and networks dominated by internal dilations are close to the η_i vertex (pink shading). Networks dominated by their in-component would be close to the η_s vertex (green shading), but none of the networks are. (c) Scatter plot with the fraction of control nodes in FC for real networks (n_{FC}) and their degree-preserving randomization ($n_{FC}^{Rand-Deg}$). The error bars denote the estimated standard deviation of the randomized ensembles. (d, e) Cycle number z-score for different cycle lengths in real versus degree-preserving randomized networks for the networks with $n_{FC} \gg n_{FC}^{Rand-Deg}$ (panel d) and $n_{FC} \ll n_{FC}^{Rand-Deg}$ (panel e).

(Table S1 and Supplementary Text). We find much weaker agreement: for most networks the number of FC control nodes is higher than the number of control nodes in randomized versions ($n_{FC} > n_{FC}^{Rand-Deg}$) (Fig. 2c). A closer look reveals that the cycle structure of the real networks is responsible for the underestimation of n_{FC} . Although the size of the largest SCC is similar or smaller compared to their degree-preserving randomized counterparts, real networks tend to have a more complicated cycle structure, evidenced by the over-representation of cycles compared to the randomized networks (Fig. 2d), and reflected by the larger size of their FVS (Table S1). A subset of networks, which includes food webs and citation networks, features fewer cycles than randomized networks and a smaller SCC than randomized networks, leading to $n_{FC} < n_{FC}^{Rand-Deg}$ (Table S1). Similarly to

the case of SC, full randomization, which turns the network into an Erdős-Rényi directed network [31], shows little correlation between n_{FC} in randomized networks and real networks (Fig. S1, Table S1, and Supplementary Text).

III. STRUCTURE-BASED CONTROL AND DYNAMIC MODELS OF REAL SYSTEMS

Validated dynamic models can be an excellent testing ground to assess control methods [5, 7, 20, S49]. Here we use two models for the gene regulatory network underlying the segmentation of the fruit fly (*Drosophila melanogaster*) during embryonic development: a differential equation model by von Dassow et al. [34] (Fig.

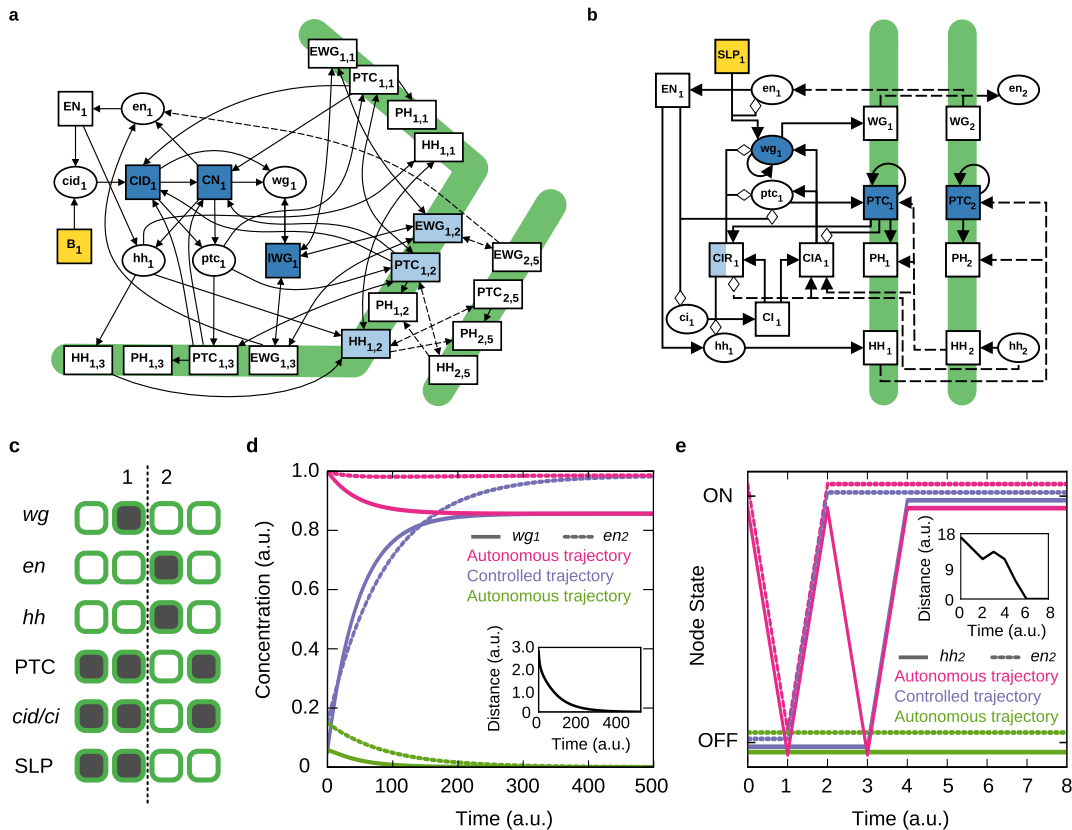


Fig. 3. Control of the *Drosophila* segment polarity network models. (a, b) Networks corresponding to the differential equation model (panel a) and the discrete model (panel b). Each figure shows one cell of the four-cell parasegment together with the cell boundaries (thick green lines); the complete networks contain four cells in a symmetric completion of each figure. Elliptical nodes denote mRNAs and rectangular nodes denote proteins, which can be localized inside the cell or in the membrane (subscripts refer to the cell number and surface index). Intracellular interactions are drawn with solid lines and intercellular interactions are dashed. In panel b, positive edges are drawn with black arrowheads and negative edges with white diamonds. Yellow nodes are source nodes, blue nodes are FC nodes in every cell, and half white/half blue nodes are FC nodes in alternating cells. Dark blue nodes are sufficient for attractor control in the considered dynamic models. (c) Wild type segment polarity gene product expression pattern in a *Drosophila* parasegment. The parasegment boundary (dotted line) is between the *wg*-expressing cells (cell 1) and *en*-expressing cells (cell 2). (d, e) The dynamics of *wg* in the first cell (panel d, solid lines) and *hh* in the second cell (panel e, solid lines), and *en* in the second cell (dotted lines) in the models. Pink lines and green lines represent autonomous trajectories that start from different initial conditions and converge to different steady states (the wild type state and the unpatterned state, respectively). Blue lines represent the case when the system starts from the initial condition that autonomously evolves to the unpatterned state, but when applying FC, evolves into the wild type steady state. Insets: evolution of the norm of the difference between the desired attractor and the controlled state trajectory using FC.

3a) and a discrete (Boolean) model by Albert and Othmer [35] (Fig. 3b). Both models consider a group of four subsequent cells as a repeating unit, include intracellular and intercellular interactions among proteins and mRNAs, and both recapitulate the observed (wild type) pattern of gene expression (Fig. 3a-c and Supplementary Text).

Using SC and FC on these network models, we find $N_{SC} = 24$ (4) and $N_{FC} = 52$ (14) for the differential equation (discrete) model (Fig. 3a-c, Fig. S2, and Supplementary Text). Both model networks are dominated by η_{FVS} (0.66 and 0.71, respectively), similarly to the brown-shaded networks in Fig. 2. For SC, the appropriate driver signal $\mathbf{u}(t)$ needs to be determined for each initial condition using, for example, minimum-energy control [18] or optimal control [9]. For FC, locking the FC

nodes in their trajectory in the wild type attractor successfully steers the system to the wild type attractor (Fig. 3d-e, Fig. S3-Fig. S5, and Supplementary Text). Thus, FC gives a control intervention which is directly applicable to dynamic models and which is directly linked to their natural long-term behavior. We emphasize that a control intervention for a real biological system would involve combining FC or SC with a closed-loop control approach because of the inherently approximate nature of any model [8, 9].

A subset of the FC node set is often sufficient for a given model and an attractor of interest [3, 22]. For the fruit fly gene regulatory models we show that 16 (12) nodes are sufficient for the continuous (discrete) model, respectively, which is a 66% (14%) reduction (Fig. 3a-c, Fig. S3-Fig. S5, and Supplementary Text). This shows

that FC provides a benchmark for attractor control node sets that are model independent, as well as an upper limit to model dependent control sets. Thus FC can be used as a gauge for the large body of recent control methods that require a dynamic model to be used [5, 7, 20, 21, S49]. To our knowledge, SC provides no analogue to this.

IV. DISCUSSION AND CONCLUSIONS

Network control methods have the general objective of identifying network elements that can manipulate a system given a specified goal and a set of constraints. Yet, as we demonstrate using SC and FC, the definition of control (e.g. full control or attractor control) and the dynamics of the system (linear or non-linear) can have a significant impact on what these network elements are and how many of them are needed.

SC and FC answer complementary aspects of control in a complex network; which one to use depends on the specific question being asked and on what the natural definition of control is in the system or discipline of interest. We argue that attractor-based control (and, thus, FC) is often the natural choice of control for systems in which the use of dynamic models is well established [23, 25–27], particularly in biological networks, in which dynamic models have a long history and an ever-increasing predictive power [27, 36]. As we showed in this work, FC is directly applicable to systems in which only structural information is known, and also to systems in which a parameterized dynamic model is available, for which it provides realizable control strategies that are robust to changes in the parameters and functions. FC also pro-

vides a benchmark and a point of contact with the large body of work in control methods that require the network structure and a dynamic model [5, 7, 18, 20, 21]. To our knowledge, something similar is not the case for SC, which instead has the advantage of being a well-developed concept in control and systems theory with connections to other notions of control in linear and non-linear systems [8, 18]. Further work is needed to extend FC and address questions such as the level of control provided by a subset of nodes and the difficulty of steering the system towards a desired state (control energy), concepts which are well-developed in control theory approaches [8, 9, 18]. Taken together, our work opens up a new research direction in the control of complex networks with nonlinear dynamics, connects the field of dynamic modeling with classical structural control theory, and has promising theoretical and practical applications.

ACKNOWLEDGMENTS

We would like to thank A. Mochizuki and M.T. Angulo for helpful discussions, and Y.Y. Liu for his generous assistance and for providing us some of the networks in this study. We would also like to thank The Mathematical Biosciences Institute for the workshop “Control and Observability of Network Dynamics”, which greatly enriched this paper. This work was supported by NSF grants PHY 1205840 and IIS 1160995. JGTZ is a recipient of a Stand Up To Cancer - The V Foundation Convergence Scholar Award. Part of this research was conducted with computational resources provided by The Institute for Cyber-Science at The Pennsylvania State University.

-
- [1] Liu, Y. Y., Slotine, J. J. & Barabási, A. L. (2011). Controllability of complex networks. *Nature*, 473(7346), 167-173.
 - [2] Nepusz, T. & Vicsek, T. (2012). Controlling edge dynamics in complex networks. *Nature Physics*, 8(7), 568-573.
 - [3] Mochizuki, A., Fiedler, B., Kurosawa, G. & Saito, D. (2013). Dynamics and control at feedback vertex sets. II: A faithful monitor to determine the diversity of molecular activities in regulatory networks. *Journal of theoretical biology*, 335, 130-146.
 - [4] Sun, J. & Motter, A. E. (2013). Controllability transition and nonlocality in network control. *Physical review letters*, 110(20), 208701.
 - [5] Corneliussen, S. P., Kath, W. L. & Motter, A. E. (2013). Realistic control of network dynamics. *Nature communications*, 4, 1942.
 - [6] Ruths, J. & Ruths, D. (2014). Control profiles of complex networks. *Science*, 343(6177), 1373-1376.
 - [7] Zañudo, J. G. T. & Albert, R. (2015). Cell fate reprogramming by control of intracellular network dynamics. *PLoS Comput Biol*, 11(4), e1004193.
 - [8] Slotine, J. J. E. & Li, W. (1991). *Applied nonlinear control* (Vol. 199, No. 1). Englewood Cliffs, NJ: Prentice-Hall.
 - [9] Kirk, D. E. (2012). *Optimal control theory: an introduction*. Dover Publications.
 - [10] Lin, C. T. (1974). Structural controllability. *Automatic Control, IEEE Transactions on*, 19(3), 201-208.
 - [11] Shields, R. W. & Pearson, J. B. (1975). Structural controllability of multi-input linear systems. *Automatic Control, IEEE Transactions on*, 21, 203-212.
 - [12] Vinayagam, A., Gibson, T. E., Lee, H. J., Yilmazel, B., Roessel, C., Hu, Y., ... and Barabási, A. L. (2015). Controllability analysis of the directed human protein interaction network identifies disease genes and drug targets. *Proceedings of the National Academy of Sciences*, 113 (18) 4976-4981.
 - [13] Kawakami, E., Singh, V. K., Matsubara, K., Ishii, T., Matsuoka, Y., Hase, T., ... and Subramanian, I. (2016). Network analyses based on comprehensive molecular interaction maps reveal robust control structures in yeast stress response pathways. *npj Systems Biology and Applications*, 2, 15018.
 - [14] Gu, S., Pasqualetti, F., Cieslak, M., Telesford, Q. K., Alfred, B. Y., Kahn, A. E., ... and Bassett, D. S. (2015). Controllability of structural brain networks. *Nature communications*, 6, 8414.
 - [15] Liu, Y. Y., Slotine, J. J. & Barabási, A. L. (2013). Observability of complex systems. *Proceedings of the National Academy of Sciences*, 110(7), 2460-2465.
 - [16] Menichetti, G., Dall’Asta, L. & Bianconi, G. (2014). Network controllability is determined by the density of low in-degree and out-degree nodes. *Physical review letters*, 113(7), 078701.
 - [17] Nacher, J. C. & Akutsu, T. (2013). Structural controllability of unidirectional bipartite networks. *Scientific reports*, 3, 1647.
 - [18] Liu, Y. Y. & Barabási, A. L. (2015). Control Principles of Complex Networks. *arXiv preprint arXiv:1508.05384*.

- [19] Müller F.J. & Schuppert A. (2011). Few inputs can reprogram biological networks. *Nature* 478, E4. doi: 10.1038/nature10543.
- [20] Wells, D. K., Kath, W. L. & Motter, A. E. (2015). Control of stochastic and induced switching in biophysical networks. *Physical Review X*, 5(3), 031036.
- [21] Murrugarra, D. & Dimitrova, E. S. (2015). Molecular network control through boolean canalization. *EURASIP Journal on Bioinformatics and Systems Biology*, 2015(1), 1-8.
- [22] Fiedler, B., Mochizuki, A., Kurosawa, G. & Saito, D. (2013). Dynamics and control at feedback vertex sets. I: Informative and determining nodes in regulatory networks. *Journal of Dynamics and Differential Equations*, 25(3), 563-604.
- [23] Allen, L. J. (2010). *An introduction to stochastic processes with applications to biology*. CRC Press.
- [24] Novozhilov, A. S., Karev, G. P., & Koonin, E. V. (2006). Biological applications of the theory of birth-and-death processes. *Briefings in bioinformatics*, 7(1), 70-85.
- [25] Daley, D. J., Gani, J. & Gani, J. M. (2001). *Epidemic modelling: an introduction* (Vol. 15). Cambridge University Press.
- [26] Tyson, J. J., Chen, K. C., & Novak, B. (2003). Sniffers, buzzers, toggles and blinkers: dynamics of regulatory and signaling pathways in the cell. *Current opinion in cell biology*, 15(2), 221-231.
- [27] Alon, U. (2006). *An introduction to systems biology: design principles of biological circuits*. CRC press.
- [28] Thomas, R. (1978). Logical analysis of systems comprising feedback loops. *Journal of Theoretical Biology*, 73(4), 631-656.
- [29] Glass, L., & Kauffman, S. A. (1973). The logical analysis of continuous, non-linear biochemical control networks. *Journal of theoretical Biology*, 39(1), 103-129.
- [30] Kramer, A. D., Guillory, J. E., & Hancock, J. T. (2014). Experimental evidence of massive-scale emotional contagion through social networks. *Proceedings of the National Academy of Sciences*, 111(24), 8788-8790.
- [31] Newman, M. (2010). *Networks: an introduction*. OUP Oxford.
- [32] Maslov, S., & Sneppen, K. (2002). Specificity and stability in topology of protein networks. *Science*, 296(5569), 910-913.
- [33] Gates, A. J., & Rocha, L. M. (2015). Control of complex networks requires both structure and dynamics. *Scientific Reports*, 6 (24456).
- [34] Von Dassow, G., Meir, E., Munro, E. M., & Odell, G. M. (2000). The segment polarity network is a robust developmental module. *Nature*, 406(6792), 188-192.
- [35] Albert, R., & Othmer, H. G. (2003). The topology of the regulatory interactions predicts the expression pattern of the segment polarity genes in *Drosophila melanogaster*. *Journal of theoretical biology*, 223(1), 1-18.
- [36] Phillips, R., Kondev, J., Theriot, J., & Garcia, H. (2012). *Physical biology of the cell*. Garland Science.
- [S1] Festa, P., Pardalos, P. M., & Resende, M. G. (1999). Feedback set problems. In *Handbook of combinatorial optimization* (pp. 209-258). Springer US.
- [S2] Even, G., Naor, J. S., Schieber, B., & Sudan, M. (1998). Approximating minimum feedback sets and multicuts in directed graphs. *Algorithmica*, 20(2), 151-174.
- [S3] Karp, R. M. (1972). Reducibility among combinatorial problems. RE Miller, JW Thatcher (Eds.), *Complexity Of Computer Computations*, Plenum Press, New York, 85-103.
- [S4] Resende, M. G. (2009). Greedy randomized adaptive search procedures greedy randomized adaptive search procedures. *Encyclopedia of optimization*, 1460-1469.
- [S5] Pardalos, P. M., Qian, T., & Resende, M. G. (1998). A greedy randomized adaptive search procedure for the feedback vertex set problem. *Journal of Combinatorial Optimization*, 2(4), 399-412.
- [S6] Festa, P., Pardalos, P. M., & Resende, M. G. (2001). Algorithm 815: FORTRAN subroutines for computing approximate solutions of feedback set problems using GRASP. *ACM Transactions on Mathematical Software (TOMS)*, 27(4), 456-464.
- [S7] Kalman, R. E. (1963). Mathematical description of linear dynamical systems. *Journal of the Society for Industrial and Applied Mathematics, Series A: Control*, 1(2), 152-192.
- [S8] Isidori, A. (2013). *Nonlinear control systems*. Springer Science & Business Media.
- [S9] Cowan, N. J., Chastain, E. J., Vilhena, D. A., Freudenberg, J. S., & Bergstrom, C. T. (2012). Nodal dynamics, not degree distributions, determine the structural controllability of complex networks. *PloS one*, 7(6), e38398.
- [S10] Zhao, C., Wang, W. X., Liu, Y. Y., & Slotine, J. J. (2015). Intrinsic dynamics induce global symmetry in network controllability. *Scientific reports*, 5.
- [S11] Gama-Castro, S., Jiménez-Jacinto, V., Peralta-Gil, M., Santos-Zavaleta, A., Peñaloza-Spinola, M. I., Contreras-Moreira, B., ... & Bonavides-Martínez, C. (2008). RegulonDB (version 6.0): gene regulation model of *Escherichia coli* K-12 beyond transcription, active (experimental) annotated promoters and Textpresso navigation. *Nucleic acids research*, 36(suppl 1), D120-D124.
- [S12] Shen-Orr, S. S., Milo, R., Mangan, S., & Alon, U. (2002). Network motifs in the transcriptional regulation network of *Escherichia coli*. *Nature genetics*, 31(1), 64-68.
- [S13] Balaji, S., Babu, M. M., Iyer, L. M., Luscombe, N. M., & Aravind, L. (2006). Comprehensive analysis of combinatorial regulation using the transcriptional regulatory network of yeast. *Journal of molecular biology*, 360(1), 213-227.
- [S14] Milo, R., Shen-Orr, S., Itzkovitz, S., Kashtan, N., Chklovskii, D., & Alon, U. (2002). Network motifs: simple building blocks of complex networks. *Science*, 298(5594), 824-827.
- [S15] Norlen, K., Lucas, G., Gebbie, M., & Chuang, J. (2002, August). EVA: Extraction, visualization and analysis of the telecommunications and media ownership network. In *Proceedings of International Telecommunications Society 14th Biennial Conference (ITS2002)*, Seoul Korea.
- [S16] Jeong, H., Tombor, B., Albert, R., Oltvai, Z. N., & Barabási, A. L. (2000). The large-scale organization of metabolic networks. *Nature*, 407(6804), 651-654.
- [S17] Watts, D. J., & Strogatz, S. H. (1998). Collective dynamics of 'small-world' networks. *Nature*, 393(6684), 440-442.
- [S18] White, J. G., Southgate, E., Thomson, J. N., & Brenner, S. (1986). The structure of the nervous system of the nematode *Caenorhabditis elegans*: the mind of a worm. *Phil. Trans. R. Soc. Lond.*, 314, 1-340.
- [S19] Huxham, M., Beaney, S., & Raffaelli, D. (1996). Do parasites reduce the chances of triangulation in a real food web? *Oikos*, 284-300.
- [S20] Dunne, J. A., Williams, R. J., & Martinez, N. D. (2002). Food-web structure and network theory: the role of connectance and size. *Proceedings of the National Academy of Sciences*, 99(20), 12917-12922.
- [S21] Christian, R. R., & Luczkovich, J. J. (1999). Organizing and understanding a winter's seagrass foodweb network through effective trophic levels. *Ecological Modelling*, 117(1), 99-124.
- [S22] Martinez, N. D., Hawkins, B. A., Dawah, H. A., & Feifarek, B. P. (1999). Effects of sampling effort on characterization of food-web structure. *Ecology*, 80(3), 1044-1055.
- [S23] Martinez, N. D. (1991). Artifacts or attributes? Effects of resolution on the Little Rock Lake food web. *Ecological Monographs*, 61(4), 367-392.
- [S24] Adamic, L. A., & Glance, N. (2005, August). The political blogosphere and the 2004 US election: divided they blog. In *Proceedings of the 3rd international workshop on Link discovery* (pp. 36-43). ACM.
- [S25] Leskovec, J., Lang, K. J., Dasgupta, A., & Mahoney, M. W. (2009). Community structure in large networks: Natural cluster sizes and the absence of large well-defined clusters. *Internet Mathematics*, 6(1), 29-123.
- [S26] Albert, R., Jeong, H., & Barabási, A. L. (1999). Internet: Diameter of the world-wide web. *Nature*, 401(6749), 130-131.

- [S27] Matei, R., Iamnitchi, A., & Foster, I. (2002). Mapping the Gnutella network. *Internet Computing*, IEEE, 6(1), 50-57.
- [S28] Leskovec, J., Kleinberg, J., & Faloutsos, C. (2007). Graph evolution: Densification and shrinking diameters. *ACM Transactions on Knowledge Discovery from Data (TKDD)*, 1(1), 2.
- [S29] Brglez, F., Bryan, D., & Kozminski, K. (1989, May). Combinational profiles of sequential benchmark circuits. In *Circuits and Systems, 1989.*, IEEE International Symposium on (pp. 1929-1934). IEEE.
- [S30] i Cancho, R. F., Janssen, C., & Solé, R. V. (2001). Topology of technology graphs: Small world patterns in electronic circuits. *Physical Review E*, 64(4), 046119.
- [S31] Bianconi, G., Gulbahce, N., & Motter, A. E. (2008). Local structure of directed networks. *Physical review letters*, 100(11), 118701.
- [S32] Leskovec, J., Huttenlocher, D., & Kleinberg, J. (2010, April). Signed networks in social media. In *Proceedings of the SIGCHI conference on human factors in computing systems* (pp. 1361-1370). ACM.
- [S33] Leskovec, J., Huttenlocher, D., & Kleinberg, J. (2010, April). Predicting positive and negative links in online social networks. In *Proceedings of the 19th international conference on World wide web* (pp. 641-650). ACM.
- [S34] Milo, R., Itzkovitz, S., Kashtan, N., Levitt, R., Shen-Orr, S., Ayzenshtat, I., ... & Alon, U. (2004). Superfamilies of evolved and designed networks. *Science*, 303(5663), 1538-1542.
- [S35] Zeleny, L. D. (1950). Adaptation of research findings in social leadership to college classroom procedures. *Sociometry*, 13(4), 314-328.
- [S36] MacRae, D. (1960). Direct factor analysis of sociometric data. *Sociometry*, 23(4), 360-371.
- [S37] Richardson, M., Agrawal, R., & Domingos, P. (2003). Trust management for the semantic web. In *The Semantic Web-ISWC 2003* (pp. 351-368). Springer Berlin Heidelberg.
- [S38] Leskovec, J., Kleinberg, J., & Faloutsos, C. (2005, August). Graphs over time: densification laws, shrinking diameters and possible explanations. In *Proceedings of the eleventh ACM SIGKDD international conference on Knowledge discovery in data mining* (pp. 177-187). ACM.
- [S39] Gehrke, J., Ginsparg, P., & Kleinberg, J. (2003). Overview of the 2003 KDD Cup. *ACM SIGKDD Explorations Newsletter*, 5(2), 149-151.
- [S40] Opsahl, T., & Panzarasa, P. (2009). Clustering in weighted networks. *Social networks*, 31(2), 155-163. Chicago
- [S41] Song, C., Qu, Z., Blumm, N., & Barabási, A. L. (2010). Limits of predictability in human mobility. *Science*, 327(5968), 1018-1021.
- [S42] Eckmann, J. P., Moses, E., & Sergi, D. (2004). Entropy of dialogues creates coherent structures in e-mail traffic. *Proceedings of the National Academy of Sciences of the United States of America*, 101(40), 14333-14337.
- [S43] Freeman, S. C., & Freeman, L. C. (1979). The networkers network: A study of the impact of a new communications medium on sociometric structure. School of Social Sciences University of Calif..
- [S44] Cross, R. L., & Parker, A. (2004). *The hidden power of social networks: Understanding how work really gets done in organizations*. Harvard Business Review Press.
- [S45] Chaves, M., Sontag, E. D., & Albert, R. (2006). Methods of robustness analysis for Boolean models of gene control networks. *IEE Proc.-Syst. Biol*, 153(4), 154.
- [S46] Von Dassow, G., & Odell, G. M. (2002). Design and constraints of the *Drosophila* segment polarity module: robust spatial patterning emerges from intertwined cell state switches. *Journal of Experimental Zoology*, 294(3), 179-215.
- [S47] Daniels, B. C., Chen, Y. J., Sethna, J. P., Gutenkunst, R. N., & Myers, C. R. (2008). Sloppiness, robustness, and evolvability in systems biology. *Current opinion in biotechnology*, 19(4), 389-395.
- [S48] Meir, E., Munro, E. M., Odell, G. M., & Von Dassow, G. (2002). Ingeneue: a versatile tool for reconstituting genetic networks, with examples from the segment polarity network. *Journal of Experimental Zoology*, 294(3), 216-251.
- [S49] Gates, A. J., & Rocha, L. M. (2015). Control of complex networks requires both structure and dynamics. *Scientific Reports*, 6 (24456).
- [S50] Akutsu, T., Hayashida, M., Ching, W. K., & Ng, M. K. (2007). Control of Boolean networks: hardness results and algorithms for tree structured networks. *Journal of Theoretical Biology*, 244(4), 670-679.
- [S51] Cheng, D., & Qi, H. (2009). Controllability and observability of Boolean control networks. *Automatica*, 45(7), 1659-1667.

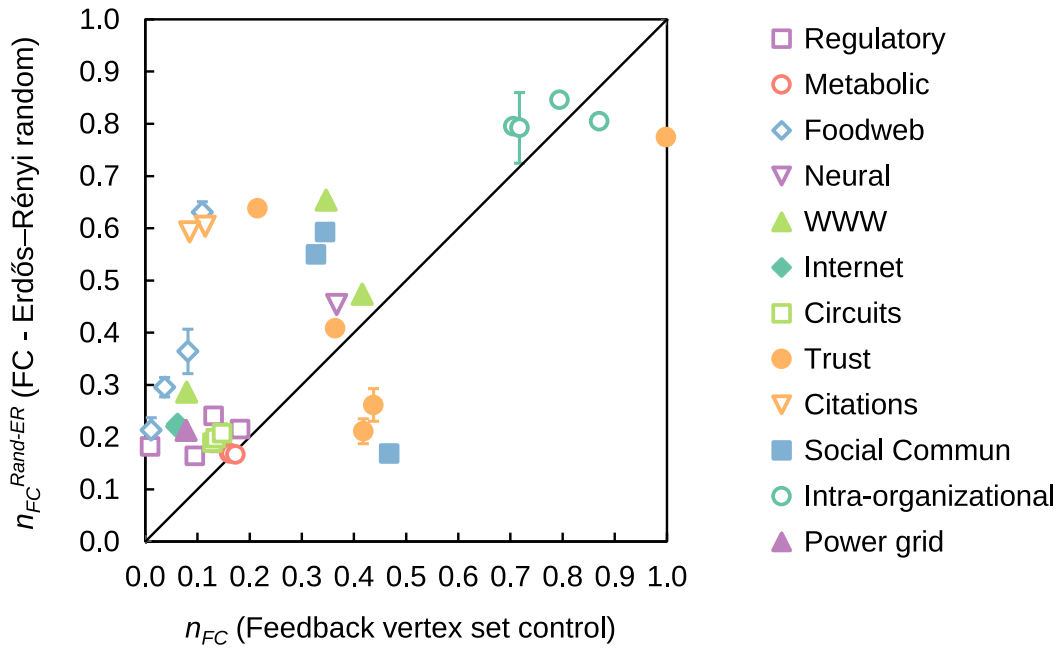


Fig. S1. Structure-based control in fully randomized networks. Scatter plot with the fraction of control nodes in feedback vertex set (FVS) control for real networks (n_{FC} , horizontal axis) and their full randomization (Erdős-Rényi, $n_{FC}^{Rand-ER}$). The bold line denotes the positions in the plot with $n_{FC} = n_{FC}^{Rand-ER}$, and the error bars denote the estimated standard deviation of the randomized network ensembles. n_{FC} in real networks shows a weak correlation with its value $n_{FC}^{Rand-ER}$ in full randomization. The intra-organizational networks at the top-right part of the plot have a large graph density and are close to being complete graphs; because of this, the feedback vertex set of these networks and their Erdős-Rényi networks is very similar (i.e., the FVS is approximately the whole graph).

Type	Name	N	M	n_{SC}	n_{FC}	$n_{FC}^{Rand-Deg}$	η_{FVS}	η_s	η_e	η_i	Cycle z-score	Relative SCC size
Regulatory	TRN Yeast 1	4441	12873	0.965	0.009	0.010	0.003	0.007	0.990	0.000	1.2	-0.248
	TRN Yeast 2	688	1079	0.821	0.141	0.140	0.002	0.170	0.818	0.010	13.1	0.913
	TRN E coli 1	1550	3340	0.891	0.095	0.036	0.065	0.035	0.900	0.000	88.4	-0.161
	TRN E coli 2	418	519	0.751	0.182	0.182	0.000	0.241	0.749	0.010	-0.3	-1.000
	US-Corps Owner.	7253	6726	0.82	0.131	0.129	0.002	0.157	0.831	0.010	43.1	0.834
Metabolic	<i>E. coli</i>	2275	5763	0.382	0.161	0.071	0.265	0.045	0.010	0.680	40.4	-0.017
	<i>S. cerevisiae</i>	1511	3833	0.329	0.164	0.082	0.292	0.061	0.000	0.647	34.6	-0.003
	<i>C. elegans</i>	1173	2864	0.302	0.173	0.089	0.315	0.077	0.000	0.608	37.3	-0.006
Neural	<i>C. elegans</i>	297	2345	0.165	0.367	0.324	0.626	0.206	0.000	0.168	19.8	-0.089
Food web	Ythan	135	601	0.511	0.037	0.095	0.055	0.014	0.699	0.233	-14.5	-0.971
	Seagrass	49	226	0.265	0.082	0.228	0.188	0.063	0.500	0.249	-12.7	-1.000
	Grassland	88	137	0.523	0.011	0.028	0.000	0.022	0.739	0.240	-1.9	-1.000
	Little Rock	183	2494	0.541	0.109	0.221	0.161	0.008	0.000	0.831	-23.1	-0.826
WWW	Political blogs	1224	19025	0.356	0.346	0.295	0.379	0.227	0.107	0.287	149.3	-0.025
	nd.edu	325729	1497134	0.677	0.080	0.114	0.105	0.000	0.762	0.133	21480.0*	-0.593
	stanford.edu	281903	2312497	0.317	0.416	0.235	0.000	0.228	0.000	0.772	31790.4*	-0.407
Internet	p2p-1	10876	39994	0.552	0.062	0.075	0.098	0.003	0.890	0.009	-4.4	-0.032
	p2p-2	8846	31839	0.578	0.060	0.074	0.075	0.021	0.885	0.019	0.5	-0.039
	p2p-3	8717	31525	0.577	0.062	0.072	0.085	0.014	0.892	0.009	4.5	-0.037
Circuits	s838	512	819	0.232	0.129	0.098	0.222	0.235	0.000	0.543	52.0	-0.644
	s420	252	399	0.234	0.135	0.111	0.214	0.241	0.000	0.545	25.7	-0.619
	s208	122	189	0.238	0.148	0.131	0.207	0.259	0.000	0.534	12.3	-0.511
Powergrid	Texas	4889	5855	0.325	0.078	0.085	0.003	0.238	0.444	0.315	1.6	-0.992
Trust	Slashdot	82168	948464	0.045	0.998	0.327	0.955	0.045	0.000	0.000	13951.8**	-0.089
	Wikivote	7115	103689	0.666	0.215	0.213	0.100	0.191	0.709	0.000	116.4	-0.012
	College student	32	96	0.188	0.438	0.363	0.599	0.333	0.000	0.068	5.4	-0.095
	Prison inmate	67	182	0.134	0.418	0.210	0.728	0.121	0.091	0.060	23.8	-0.264
	Epinions	75879	508837	0.549	0.364	0.365	0.224	0.288	0.155	0.332	2569.3**	-0.080
Citations	Arxiv HepTh	27770	352807	0.216	0.115	0.273	0.074	0.419	0.290	0.218	-51.5	-0.626
	Arxiv HepPh	34546	421578	0.232	0.085	0.242	0.064	0.279	0.459	0.198	-10.3	-0.492
Social Commun.	UCLonline	1899	20296	0.323	0.328	0.214	0.487	0.031	0.426	0.056	318.3	-0.006
	cellphone	36595	91826	0.204	0.468	0.184	0.657	0.128	0.000	0.214	23489.0	-0.290
	emails	3188	39256	0.426	0.345	0.269	0.343	0.188	0.179	0.290	683.9	0.010
Organizational	Freemans-2	34	830	0.029	0.794	0.747	0.965	0.000	0.000	0.035	7.8	0.000
	Freemans-1	34	695	0.029	0.706	0.658	0.961	0.000	0.000	0.039	10.0	0.000
	Manufacturing	77	2228	0.013	0.870	0.705	0.985	0.015	0.000	0.000	141.4	0.000
	Consulting	46	879	0.043	0.717	0.703	0.939	0.061	0.000	0.000	45.0	-0.023

Table S1. Network and control properties of the real networks analyzed. For each network, we show its number of nodes (N), number of directed edges (M), the fraction of nodes to be controlled under structural controllability (SC) (n_{SC}), the fraction of feedback vertex set control (FC) nodes (n_{FC}), the average fraction of FC nodes in degree-preserving randomized networks ($n_{FC}^{Rand-Deg}$), the normalized fraction of feedback vertex set (η_{FVS}), source (η_s), external (η_e), and internal (η_i) control nodes, the sum of the cycle number z-scores, and the relative strongly connected component size with respect to the randomized networks. The second page of the table shows the fraction of feedback vertex set nodes (n_{FVS}), the fraction of source nodes (n_s), the fraction of external nodes (n_e), the fraction of internal nodes (n_i), the average fraction of FC nodes in fully randomized (Erdős-Rényi) networks ($n_{FC}^{Rand-ER}$), the number of nodes in the strongly connected component (SCC) in the real networks and in degree-preserving networks. The second and third pages of the table show the number of 1-cycles, 2-cycles, 3-cycles, and 4-cycles in real networks, and the mean and standard deviation (S.D.) of the cycle numbers in degree-preserving randomized networks. The relative SCC size is calculated using $(SCC_{real} - SCC_{Rand-Deg})/SCC_{Rand-Deg}$. The z-score of each cycle number is calculated using $(C_L^{Real} - C_L^{Rand})/\sigma_{C_L}$, where C_L^{Real} is the number of L-cycles in the real network, C_L^{Rand} is the mean number of cycles in degree-preserving randomized networks, and σ_{C_L} is the standard deviation of the number of cycles. (*) The cycle z-score is larger than the number shown; the number of cycles in the real network exceeded 2×10^6 . (**) The maximum cycle length used was 3 instead of 4 because of the large number of cycles in both the real and randomized networks. (***) For these networks there were multiple SCC of similar sizes. The SCC size shown is the sum of sizes of all the SCCs.

Type	Name	n_{FVS}	n_s	n_e	n_i	$n_{FC}^{Rand-ER}$	SCC <i>real</i>	SCC <i>Rand-Deg</i>	1-cycles <i>real</i>	1-cycles <i>Rand-Deg</i>	1-cycles S.D. <i>Rand-Deg</i>
Regulatory	TRN Yeast 1	0.002	0.007	0.958	0.000	0.182	60	79.8	0	0.00	0.00
	TRN Yeast 2	0.001	0.140	0.670	0.008	0.188	3	0.3	0	0.00	0.00
	TRN E coli 1	0.062	0.033	0.858	0.000	0.164	15***	17.9	96	1.89	1.17
	TRN E coli 2	0.000	0.182	0.565	0.008	0.215	0	0.3	0	0.00	0.00
	US-Corps Owner.	0.002	0.129	0.684	0.008	0.240	5	0.8	2	0.59	0.76
Metabolic	<i>E. coli</i>	0.138	0.023	0.005	0.353	0.169	2105	2141.9	0	0.00	0.00
	<i>S. cerevisiae</i>	0.136	0.028	0.000	0.301	0.169	1415	1418.6	0	0.00	0.00
	<i>C. elegans</i>	0.139	0.034	0.000	0.268	0.167	1080	1086.2	0	0.00	0.00
Neural	<i>C. elegans</i>	0.276	0.091	0.000	0.074	0.454	239	262.4	0	0.00	0.00
Food web	Ythan	0.030	0.007	0.378	0.126	0.296	2	69.4	4	5.20	1.99
	Seagrass	0.061	0.020	0.163	0.081	0.364	0	36.1	3	3.86	1.79
	Grassland	0.000	0.011	0.386	0.125	0.213	0	5.6	0	0.00	0.00
	Little Rock	0.104	0.005	0.000	0.536	0.631	29***	166.6	18	11.87	3.25
WWW	Political blogs	0.217	0.130	0.061	0.164	0.654	793	813.3	3	30.61	4.27
	nd.edu	0.080	0.000	0.577	0.100	0.286	53968	132712.5	0	0.00	0.00
	stanford.edu	0.344	0.072	0.000	0.244	0.474	150532	253742.1	0	0.00	0.00
Internet	p2p-1	0.060	0.002	0.544	0.006	0.225	4317	4457.6	0	0.00	0.00
	p2p-2	0.047	0.013	0.551	0.012	0.220	3234	3366.8	0	0.00	0.00
	p2p-3	0.053	0.009	0.562	0.006	0.221	3226	3351.5	0	0.00	0.00
Circuits	s838	0.063	0.066	0.000	0.153	0.189	153***	430.0	0	0.00	0.00
	s420	0.063	0.071	0.000	0.161	0.198	77***	202.0	0	0.00	0.00
	s208	0.066	0.082	0.000	0.169	0.207	39***	79.8	0	0.00	0.00
Powergrid	Texas	0.001	0.078	0.145	0.103	0.213	13***	1626.5	0	0.00	0.00
Trust	Slashdot	0.953	0.045	0.000	0.000	0.774	71307	78297.5	78303	91.51	8.49
	Wikivote	0.074	0.141	0.524	0.000	0.638	1300	1315.4	0	0.00	0.00
	College student	0.281	0.156	0.000	0.032	0.262	23	25.4	0	0.00	0.00
	Prison inmate	0.358	0.060	0.045	0.030	0.211	39	53.0	0	0.00	0.00
	Epinions	0.159	0.205	0.110	0.236	0.407	32223	35030.6	0	0.00	0.00
Citations	Arxiv HepTh	0.017	0.098	0.068	0.051	0.604	7464	19933.8	39	20.67	3.73
	Arxiv HepPh	0.016	0.069	0.114	0.049	0.593	12711	25006.7	44	16.46	4.18
Social Commun.	UCLonline	0.308	0.019	0.270	0.036	0.550	1294	1301.6	0	0.00	0.00
	cellphone	0.392	0.076	0.000	0.128	0.169	21518	30327.7	0	0.00	0.00
	emails	0.223	0.122	0.116	0.188	0.593	2025	2004.5	0	0.00	0.00
Organizational	Freemans-2	0.794	0.000	0.000	0.029	0.846	34	34.0	0	0.00	0.00
	Freemans-1	0.706	0.000	0.000	0.029	0.795	34	34.0	0	0.00	0.00
	Manufacturing	0.857	0.013	0.000	0.000	0.805	76	76.0	0	0.00	0.00
	Consulting	0.674	0.043	0.000	0.000	0.792	43	44.0	2	21.26	2.44

Table S1. Continuation of Table S1.

Name	2-cycles real	2-cycles Rand-Deg	2-cycles S.D. Rand-Deg	3-cycles real	3-cycles Rand-Deg	3-cycles S.D. Rand-Deg	4-cycles real	4-cycles Rand-Deg	4-cycles S.D. Rand-Deg
TRN Yeast 1	9	5.64	2.46	13	12.88	3.74	29	31.01	8.694
TRN Yeast 2	1	0.06	0.26	1	0.01	0.10	0	0.00	0.045
TRN E coli 1	10	1.75	1.21	4	1.91	1.39	1	2.28	1.866
TRN E coli 2	0	0.04	0.20	0	0.01	0.10	0	0.00	0.000
US-Corps Owner.	13	0.23	0.44	2	0.06	0.24	1	0.05	0.218
<i>E. coli</i>	136	75.80	7.59	0	495.03	43.76	21442	3896.90	400.365
<i>S. cerevisiae</i>	26	51.40	6.31	0	290.24	27.52	12587	1890.78	217.395
<i>C. elegans</i>	22	37.34	5.17	0	180.08	20.57	7483	982.10	132.627
<i>C. elegans</i>	197	55.72	6.36	431	374.47	21.11	1992	2794.97	158.065
Ythan	1	15.69	3.11	0	47.75	9.54	0	162.46	38.920
Seagrass	0	7.70	1.99	0	19.28	4.67	0	53.00	12.608
Grassland	0	0.48	0.64	0	0.38	0.60	0	0.21	0.454
Little Rock	42	62.05	6.43	137	439.07	28.78	393	3477.90	270.563
Political blogs	2307	503.63	16.84	18481	10460.88	270.00	339454	237762.00	5362.960
nd.edu	379571	931.91	25.72	>2000000	26738.39	298.34	>2000000	862849.50	7850.500
stanford.edu	319861	180.04	14.27	689426	2261.60	86.61	>2000000	31871.60	1348.996
p2p-1	0	10.40	3.49	33	31.01	5.74	85	102.96	10.251
p2p-2	0	9.39	2.93	34	25.87	4.72	105	85.58	9.819
p2p-3	0	8.86	3.16	40	26.80	5.57	137	85.66	10.335
s838	0	1.18	1.05	40	1.17	1.22	23	1.25	1.023
s420	0	1.16	0.99	20	1.03	1.04	11	1.18	1.135
s208	0	1.00	1.07	10	0.96	0.99	5	1.00	0.970
Texas	0	1.05	0.91	3	0.72	0.83	1	0.96	1.086
Slashdot	365931	5962.44	76.51	493487	414775.30	2420.23	>2000000	>2000000	NA
Wikivote	2927	920.15	28.06	41856	25782.50	543.22	1104831	790962.00	20559.181
College student	16	4.72	1.88	14	9.29	2.19	9	18.07	3.362
Prison inmate	40	4.68	2.46	28	8.71	2.50	24	16.68	4.292
Epinions	103097	2904.37	48.08	740310	146423.86	1223.13	>2000000	>2000000	NA
Arxiv HepTh	483	222.24	16.10	522	3074.18	76.26	2498	48068.08	1164.529
Arxiv HepPh	657	119.64	11.50	506	1251.04	34.53	870	14502.94	324.466
UCionline	6458	621.98	17.58	10932	14291.28	210.11	383109	367359.50	6481.181
cellphone	34973	8.55	2.23	19803	26.77	5.57	41349	83.57	9.706
emails	7399	691.00	13.65	37693	16924.00	191.38	816457	461084.20	4226.713
Freemans-2	356	334.17	3.33	5416	5385.59	14.39	95082	95285.99	235.406
Freemans-1	280	251.33	3.39	3503	3466.83	16.74	52347	52531.32	276.189
Manufacturing	887	498.55	7.98	13706	10206.85	68.29	275530	229977.75	1098.990
Consulting	327	213.97	5.23	3492	2804.78	35.27	47296	40089.76	613.150

Table S1. Continuation of Table S1.

SUPPLEMENTARY TEXT

I. Feedback vertex set control

I.A. Previous work on feedback vertex set control

In [3, 22], Mochizuki, Fiedler et al. introduced the mathematical framework underlying feedback vertex set control (FC). Here we give a brief overview of the main concepts and results of [22] and its relation the work presented here. In the following $X_i(t)$, $i = 1, 2, \dots, N$, denotes the state of the variable associated to node i at time t , and $\mathbf{X} = (X_1, X_2, \dots, X_N)$ is a vector composed of the state of the variables of the network. In addition, we use X_J to denote X_j where $j \in J \subseteq \{1, 2, \dots, N\}$.

Let each of the system's node states $X_i(t)$ evolve in time according to the differential equations

$$\frac{dX_i}{dt} = F_i(X_i, X_{I_i}, t), \quad i = 1, 2, \dots, N, \quad (\text{S1})$$

where $F_i(X_i, X_{I_i}, t)$ encodes the network structure; I_i defines the predecessor (regulator) nodes of node i in the network and is such that I_i contains node i only if $\partial F_i / \partial X_i \geq 0$. In other words, negative self-regulation ($\partial F_i / \partial X_i < 0$) is not included in I_i , only positive self-regulation is ¹. Additionally, F_i and its first derivatives are assumed to be continuous functions and are assumed to be such that $\mathbf{X}(t)$ is bounded ($|\mathbf{X}(t)| < C$ for some constant C) for any finite initial condition $\mathbf{X}(t_0)$ and for all $t \geq t_0$, including the limit $t \rightarrow \infty$. Note that Eq. S1 determines the dynamics of all node variables, including source nodes, which stands in contrast to Eqs. 1-2 in the main text (Eqs. S3-S4). We consider the more general case of Eqs. 1-2 in Section I.B.

The boundedness conditions listed in the previous paragraph makes this system a so-called dissipative dynamical system, and guarantee that any initial state will converge to a global attractor \mathcal{A} as $t \rightarrow \infty$,

$$\mathcal{A} = \left\{ \mathbf{X}(0) \mid \sup_{t \in \mathbb{R}} |\mathbf{X}(t)| < \infty \right\}. \quad (\text{S2})$$

The global attractor \mathcal{A} is bounded and invariant under Eq. S1, and contains all bounded dynamical attractors: steady states, limit cycles, quasi-periodic orbits, and bounded chaotic trajectories.

For the system we consider, the following theorem (Theorem 1.3 in [22]) forms the basis of FC:

¹ Note that considering only positive self-regulation as part of I_i is equivalent to adding a new auxiliary variable ζ_i to encode for positive self-regulation (if any) and not including i as part of I_i . In other words, if $\partial F_i / \partial X_i \geq 0$ with $i \notin I_i$, then we introduce $\zeta_i = X_i$ and set $\tilde{F}_i = F_i(\zeta_i, X_{I_i}, t) + \zeta_i - X_i$ as the new equation for node i . This would make $\partial \tilde{F}_i / \partial X_i < 0$ for the expanded system and would make the feedback vertex set of the expanded system always include X_i or ζ_i . This approach of adding an auxiliary variable is used in [3, 22].

Theorem. Consider a differential equation system governed by Eq. S1 with dissipative functions F_i , and the associated directed graph G obtained from the I_i . We also assume F_i and its derivatives to be continuous. Moreover, G can contain a self-loop only if F_i does not satisfy the decay condition $\partial F_i / \partial X_i < 0$. Then a possibly empty subset $J \subseteq \{1, 2, \dots, N\}$ of vertices of G , and any two solutions \mathbf{X} and $\tilde{\mathbf{X}}$ of Eq. S1 satisfy

$$\lim_{t \rightarrow \infty} \left(X_J(t) - \tilde{X}_J(t) \right) \rightarrow 0 \quad \text{implies} \\ \lim_{t \rightarrow \infty} \left(\mathbf{X}(t) - \tilde{\mathbf{X}}(t) \right) \rightarrow \mathbf{0}$$

for all choices of nonlinearities F_i if and only if J is a feedback vertex set (FVS) of the graph G .

A consequence of this theorem is that a system governed by Eq. S1 with an empty FVS must have any pair of solutions approach each other as $t \rightarrow \infty$, i.e., there is single dynamical attractor. Now, if we take a system with a non-empty FVS and override the dynamics of its FVS with the trajectory in one of its dynamical attractors \mathcal{D} , then the overridden system is equivalent to a system with an empty FVS ². Since the dynamical attractor \mathcal{D} is still a dynamical attractor of the overridden system, which has an empty FVS, it must be the only dynamical attractor the overridden system. Hence, if we override the dynamics of the FVS of system Eq. S1 with the trajectory in one of its dynamical attractors, this theorem guarantees that the overridden system will converge to this attractor. Furthermore, overriding the full FVS is necessary and sufficient if one wants this control strategy to hold for all choices of F_i 's.

I.B. Feedback vertex set control for general system dynamics

Consider the general system used in the main text. The state of the system's N nodes at time t , characterized by source node variables $S_j(t)$ (for nodes with no incoming edges) and internal node variables $X_i(t)$, obeys the equations

$$\frac{dX_i}{dt} = F_i(X_i, X_{I_i}, t), \quad i = 1, 2, \dots, N - N_s, \quad (\text{S3})$$

$$S_j(t) = E_j(t), \quad j = N - N_s + 1, \dots, N. \quad (\text{S4})$$

The dynamics of each source node j is determined by an environmental signal $E_j(t)$, while the dynamics of each

² Let $J \subseteq \{1, 2, \dots, N\}$ be the node indices of a FVS, and let $K = \{1, 2, \dots, N\} / J$ be the node indices of nodes not in the FVS. The dynamics of nodes K in the overridden system are given by $\dot{X}_k = F'_k(X_k, X_{I'_k}, t) = F_k(X_k, X_{I_k}, t) |_{X_J(t)=X_J^{\mathcal{D}}(t)}$, $k \in K$, where $X_J^{\mathcal{D}}(t)$ is the trajectory of the overridden node states. Since $F'_k(X_k, X_{I'_k}, t) = F_k(X_k, X_{I_k}, t) |_{X_J(t)=X_J^{\mathcal{D}}(t)}$, then I'_k does not contain any node in J and the graph defined by the I'_k will have no cycles (removing J , by definition, makes the graph acyclic).

internal node i is governed by $F_i(X_i, X_{I_i}, t)$, where the I_i determines the predecessor nodes of i and satisfies the same conditions as in Section I.A. The dynamics are assumed to be bounded, and the F_i 's and E_j 's and their first derivatives are taken to be continuous.

For this system, the theorem in Section I.A and its consequences (i.e., the results of refs. [3, 22]) cannot be applied directly since the source node variables $S_j(t)$ do not obey Eq. S1. Note that the addition of the environmental signals E_j is not merely cosmetic; the E_j 's denote stimuli the system obtains from its environment through the source nodes; these stimuli can affect the dynamical attractors available to the system (e.g. steady states can merge or disappear if E_j is fixed at different values).

Here we extend the previous results of feedback vertex set control to the more general system dynamics. Let \mathcal{D} be the desired dynamical attractor and let $E_j^{\mathcal{D}}(t)$ be the external signals in which this attractor is obtained. Now, assume that the system's source nodes are driven by an arbitrary $E_j(t)$. If starting at time t_0 , we override the state of the source nodes $S_j(t)$ with $E_j^{\mathcal{D}}(t)$, then for $t > t_0$ we will have $S_j(t)$ be in their state in \mathcal{D} . Additionally, the dynamics of the X_i for $t > t_0$ can be described by $\dot{X}_i = F'_i(X_i, X_{I'_i}, t) = F_i |_{S_j(t)=E_j^{\mathcal{D}}(t)}$, where the F'_i no longer depend on S_j (i.e., I'_i is I_i with all the S_j removed). Since the dynamics of the modified system now obey Eq. S1 (with F'_i instead of F_i), then we can guarantee that the FVS can be used to steer the system to any dynamical attractor of interest. Finally, since $F'_i = F_i |_{S_j(t)=E_j^{\mathcal{D}}(t)}$, then \mathcal{D} is one of the attractors of the modified system ($\dot{X}_i = F'_i$ and $\dot{X}_i = F_i$ with $S_j(t) = E_j^{\mathcal{D}}(t)$ both have the same governing equations). The result is that the overriding the state of the source nodes S_j and of the FVS into the state in a dynamical attractor \mathcal{D} is guaranteed to steer the system to \mathcal{D} as $t \rightarrow \infty$.

I.C. Identifying the minimal feedback vertex set control set of a network

The FC node set of a network of N nodes is composed of the source nodes of the network (N_s of them) and of the FVS of the network. The minimal FC node set N_{FC} of a network is obtained by finding a minimal FVS, since the number of source nodes N_s is fixed for any given network. The minimal FVS of a network is not guaranteed to be unique, and is often found to have a large degeneracy (see the examples in Fig. 1 of the main text).

In order to find the minimal FVS control set of a network, we must find which of the possible 2^{N-N_s} node sets is a minimal FVS. The problem of identifying the minimal FVS has a long history in the area of circuit design [S1] and a variety of fast algorithms exist to find close-to-minimal solutions [S1, S2] even though solving the minimal FVS problem exactly is NP-hard [S3]. Here we use the FVS adaptation of a heuristic algorithm known as the greedy randomized adaptive search procedure (GRASP) [S4], which is commonly used for combinatorial optimiza-

tion problems [S1].

GRASP is an iterative procedure in which each iteration consists of two phases: a construction phase in which a feasible solution to the problem is produced based on a greedy measure and a randomized selection process (given a cutoff for the greedy measure, a feasible solution below the cutoff is chosen randomly and uniformly), and a local search phase in which the local neighborhood in the space of solutions is explored to find a local minimum of the problem. The FVS adaptation of GRASP incorporates the wiring diagram of the network into the procedure by using the in-degree and out-degree of each node as the greedy measure in the construction phase and by utilizing a graph reduction technique that preserves the FVS during the local search phase [S5, S6]. In addition, we preprocess all networks by iteratively removing source and sink nodes (this is done iteratively because new source/sink nodes may appear after a source/sink node is removed), since a minimal FVS of a network is invariant under removing nodes that do not participate in directed cycles.

For this work, we use a custom code in Python to iteratively remove source and sink nodes in each network analyzed. The resulting network is then used as an input to the FORTRAN implementation of the FVS adaptation of GRASP [S5, S6] using the default settings (2048 iterations and a random uniformly chosen cutoff for the randomized selection process in each iteration), unless otherwise noted.

II. Structural controllability

II.A. Notes on structural controllability

In structural controllability (SC) we consider a system with an underlying network structure whose autonomous dynamics are governed by linear time-invariant ordinary differential equations

$$\frac{d\mathbf{x}}{dt} = \mathbf{A}\mathbf{x}(t), \quad (\text{S5})$$

where $\mathbf{x}(t) = (x_1(t), x_2(t), \dots, x_N(t))$ denotes the state of the system, and \mathbf{A} is a $N \times N$ matrix that encodes the network structure and is such that a_{ik} is nonzero only if there is a directed edge from k to i . Given this system, SC's aim is to identify external driver node signals $\mathbf{u}(t) = (u_1(t), \dots, u_M(t))$ that can steer the system from any initial state to any final state in finite time (i.e., full control), and that are coupled to Eq. S5 in the following way (Eq. 3 in the main text)

$$\frac{d\mathbf{x}}{dt} = \mathbf{A}\mathbf{x}(t) + \mathbf{B}\mathbf{u}(t), \quad (\text{S6})$$

where \mathbf{B} is a $N \times M$ matrix that describes which nodes are driven by the external signals $\mathbf{u}(t)$.

The work of Lin, Shields, Pearson, and others showed that if such a system can be controlled in the specified

way by a given pair (A, B) , which can be verified using Kalman's controllability rank condition ³, this will also be true for almost all pairs (A, B) (except for a set of measure zero) [8, 10, 11]. In other words, SC is necessary and sufficient for control of almost all linear time-invariant systems consistent with the network structure in A . The applicability of SC also extends to nonlinear systems; SC of the linearized nonlinear system around a state of interest x^* is a sufficient condition for (local) controllability of the system from x^* to any sufficiently close state in a sufficiently small time [8, 18, S8] (the same is also true if we are interested in a trajectory instead of single state x^*). Furthermore, SC of the linearized nonlinear system is also a sufficient condition for some nonlinear notions of controllability such as accessibility [8, 18, S8].

II.B. Structural controllability and self-dynamics

In a system governed by Eq. S6, self-dynamics is captured by having the matrix elements in the diagonal of A be nonzero (i.e., a self-loop in the network structure). If each node variable in the system has self-dynamics, then every node in the associated graph structure of A will have a self-loop. Directly applying SC to such a graph will yield the surprising result that a single driver signal $\mathbf{u}(t) = (u_1(t))$ is necessary and sufficient for full control, regardless of any other aspect of the graph structure [1, 18, S9]. This result, although mathematically correct, gives little insight into the impact of the underlying network structure of A (other than self loops) on control-related questions. Furthermore, as Sun et al. showed using minimal-energy control driver signals ⁴, the required driver signal $\mathbf{u}(t) = (u_1(t))$ might be numerically impossible to implement unless the number of control nodes is significantly increased [4].

We should emphasize that controllability of a system with self-dynamics by a single driver signal is a consequence of SC's assumption that each nonzero entry in A and B is independent of each other. Thus, if one considers SC for the set of (A, B) 's in which the diagonal elements of A are fixed (i.e., the self-dynamics are fixed but the every other nonzero entry is still arbitrary) then the number of driver nodes can be obtained from the eigenvalues of A and their geometric multiplicities ⁵, as shown in a recent study by Zhao et al. [S10]. For most cases, obtaining the eigenvalues of A and their geometric multiplicities is computationally demanding and requires specifying a value for the weight a_{ii} of each self-loop. For the special case of a single fixed weight α for

the self-dynamics of every node ($a_{ii} = \alpha, \forall i$), the number of driver nodes is equivalent to the one specified by SC using A but setting all diagonal elements to zero [S10].

These considerations about self-dynamics are crucial when using SC on the nonlinear systems we consider, Eqs. S3-S4. Since the nonlinear functions F_i have a decay term that prevents the system from increasing without bounds, then a linearization of the F_i 's will give nonzero diagonal entries for A . Thus, SC would predict that a single driver signal is sufficient for controllability regardless of the topology of the real network considered, a result which tells us little about structure-based control in these networks. Instead, we follow the approach of Liu et al. [1] and do not include the decay self-dynamics as a self-loop in the graph structure. Two equivalent interpretations of this approach under SC are that (i) we consider the decay terms to not dominate the linearized dynamics (i.e., we set them to zero), or (ii) every element has the same (or very similar) fixed weight for its self-dynamics (i.e., the self-dynamics are fixed and every other nonzero entry in A is arbitrary).

I.C. Identifying the minimum number of driver nodes in structural controllability

Here we use the maximum matching approach of Liu et al. [1] to identify the minimum number of driver nodes in SC. Given a directed network, an undirected bipartite graph is created in the following way: for every node i in the original network, a node i^+ of type + and a node i^- of type - are created in the bipartite graph. The connectivity in the bipartite graph is such that if node i has a directed edge to node j in the original network, then the bipartite graph will have an undirected edge from node i^+ to node j^- . As Liu et al. showed, a maximum matching of the bipartite graph (maximum number of edges with no common nodes) gives the minimum number of driver nodes in SC; each node in the original network corresponding to a node of type + that is not in the maximum matching must be directly regulated by a driver node. A maximum matching of a graph is not unique, which implies that the set of nodes that must be directly regulated by a driver node is not unique either. The maximum matching of a bipartite graph can be efficiently found in $O(\sqrt{NM})$ time using the Hopcroft-Karp algorithm.

For this work, we use a custom code in Python to implement the maximum matching approach of Liu et al. [1], and use the implementation of the Hopcroft-Karp algorithm in the Python package NetworkX (<https://networkx.github.io/>, version 1.10) to find the maximum matching.

³ Namely, that the $N \times NM$ matrix $(B, AB, A^2B, \dots, A^{N-1}B)$ has full rank, i.e., $\text{rank}(C) = N$ [S7].

⁴ Minimal-energy control driver signals are the ones that minimize the functional $\int_0^{t_f} \|\mathbf{u}(t)\|^2 dt$, where t_f is the desired final time.

⁵ The geometric multiplicity $\mu(\lambda)$ of an eigenvalue λ of A is given by $\mu(\lambda) = N - \text{rank}(\lambda I - A)$, where I is the $N \times N$ identity matrix.)

III. Structure-based control of real networks

III.A. Real networks used in this study

Here we describe each network in Table S1, provide the reference where each network was first reported, and give the link to where the network was obtained (if publicly available). For many of these networks, the orientation of the directed edges does not match the expected direction of influence in a dynamic model; if there is an edge from node i to node j , we expect the state of node i to influence the state of node j (e.g., in an epidemic model, if individual i is infected and i can spread the disease to j , then we expect node j to get infected). For these networks, we follow [1] and [6], and reverse the orientation of the directed edges in order for it to match the expected directionality of influence.

- ***E. coli* transcription regulatory network 1 [S11]**. Graph of the transcriptional regulation network in the bacterium *Escherichia coli*. Vertices denote genes; a gene that codes for a transcription factor that regulates the transcription of a target gene is denoted by a directed edge between them. The version of the network used was obtained directly from Yang-Yu Liu.
- ***E. coli* transcription regulatory network 2 [S12]**. Graph of the transcriptional regulation network in the bacterium *Escherichia coli*. Operons (a gene or group of genes transcribed together) are denoted by vertices; an operon that codes for a transcription factor that directly regulates a target operon is denoted by a directed edge. This network was obtained from Hawoong Jeong’s website <http://stat.kaist.ac.kr/index.php>.
- ***S. cerevisiae* transcription regulatory network 1 [S13], 2 [S14]**. Graph of the transcriptional regulation network in the yeast *Saccharomyces cerevisiae*. Genes are denoted by vertices; a gene that codes for a transcription factor that regulates a target gene is denoted by a directed edge between them. Network 1 was obtained from the supplemental information in ref. [S13], and network 2 was obtained from Uri Alon’s website <https://www.weizmann.ac.il/mcb/UriAlon/download/collection-complex-networks>.
- **US corporate ownership [S15]**. Graph of the ownership relations among companies in the telecommunications and media industries in the United States. Companies are denoted by vertices and ownership of a company by another is denoted by an edge originating from the owner company. This network was obtained from the Pajek network dataset <http://vlado.fmf.uni-lj.si/pub/networks/data/econ/Eva/Eva.htm>
- ***E. coli*, *S. cerevisiae*, *C. elegans* metabolic networks [S16]**. Graph of the metabolic network of the bacterium *Escherichia coli*, the yeast *Saccharomyces cerevisiae*, and the worm *Caenorhabditis elegans*. Substrates (molecules) and temporary complexes are denoted by vertices; substrates that participate as a reactant in the reaction associated to a complex have an edge to it, and substrates that are products of the reaction associated to a complex have an edge from it. These network were obtained from Hawoong Jeong’s website <http://stat.kaist.ac.kr/index.php>.
- ***C. elegans* neural network [S17, S18]**. Graph of the *Caenorhabditis elegans* worm’s neural network. Neurons are denoted by vertices and synapse/gap junctions between neurons are denoted by edges. This network was obtained from the UC Irvine Network Data Repository <http://networkdata.ics.uci.edu/data/celegansneural/>.
- **Ythan [S19, S20], Seagrass [S21, S20], Grassland [S22, S20], and Little Rock [S23, S20] food web networks**. Graph of the predatory interactions among species in the Ythan Estuary, the St. Marks Seagrass, the England/Wales Grassland, and the Little Rock Lake. Every species is denoted by a vertex, and if a species preys on another species an edge is drawn from the prey to the predator. This network was obtained from the Cosin Project network data <http://www.cosinproject.eu/extra/data/foodwebs/WEB.html>.
- **Political Blogs [S24]**. Graph of the hyperlinks between blogs on US politics in 2005. Every blog is denoted by a vertex and hyperlinks are denoted by edges that point towards the linked blog. In this work we reverse the edges of this network so that they match the direction of influence in a dynamic model (i.e., if a blog has a hyperlink to another blog, then the latter influenced the former). This network was obtained from Mark Newman’s website <http://www-personal.umich.edu/mejn/netdata/>.
- **WWW network of stanford.edu [S25] and nd.edu [S26]**. Graph of the web networks of Stanford University (domain stanford.edu) and the University of Notre Dame (domain nd.edu). Every webpage is denoted by a vertex and hyperlinks are denoted by edges that point towards the linked webpage. This network was obtained from the Stanford Large Network Dataset Collection <https://snap.stanford.edu/data/>.
- **Internet networks [S27, S28]**. Graphs of the Gnutella peer-to-peer file sharing network from August 2002; each graph represents a different snapshot of the Gnutella network. Every host is de-

- noted by a vertex and a connection from one host to another is denoted by an edge that points towards the latter. These networks were obtained from the Stanford Large Network Dataset Collection <https://snap.stanford.edu/data/>.
- **Electronic Circuits [S14, S29, S30]**. Network representations of electronic circuits from the IS-CAS89 benchmark collection. Logic gates and flip-flops are represented by vertices, and the directed connections between them are denoted edges. These networks were obtained from Uri Alon’s website <https://www.weizmann.ac.il/mcb/UriAlon/download/collection-complex-networks>.
 - **Texas power grid [S31]**. Network representation of the Texas power grid. Substations, generators, and transformers are represented by vertices, and transmission lines between them are denoted by edges, with the edge directionality corresponding to the electric power flow. This network was obtained directly from Yang-Yu Liu.
 - **Slashdot [S25]**. Friend/foe network of the technology-related news website Slashdot obtained in 2009. Users are denoted by vertices, and a user tagging another user as a friend/foe is denoted by an edge pointing towards the latter user. In this work we reverse the edges in this network so that they match the direction of influence in a dynamic model (i.e., if a user tags another user, the latter has an influence on the former). This network was obtained from the Stanford Large Network Dataset Collection <https://snap.stanford.edu/data/>.
 - **Wikivote [S32, S33]**. Who-votes-for-whom network of Wikipedia users for administrator elections. Users are denoted by vertices, and a user voting for another user is denoted by an edge pointing towards the latter user. In this work we reverse the edges of this network so that they match the direction of influence in a dynamic model (i.e., if a user votes for another user, the latter has an influence on the former). This network was obtained from the Stanford Large Network Dataset Collection <https://snap.stanford.edu/data/>.
 - **College student and prison inmate trust networks [S34, S35, S36]**. Social networks of positive sentiment of college students in a course about leadership and of inmates in prison. Each person is denoted by a vertex, and the expression of a positive sentiment of a person towards another person (based on a questionnaire) is denoted by an edge pointing towards the latter. In this work we reverse the edges of this network so that they match the direction of influence in a dynamic model (i.e., if a person has a positive sentiment towards another, the latter has an influence on the former). These networks were obtained from Uri Alon’s website <https://www.weizmann.ac.il/mcb/UriAlon/download/collection-complex-networks>.
 - **Epinions [S37]**. Who-trusts-whom online social network of Epinions.com, a general consumer review site. Users are denoted by vertices, and a user trusting another user is denoted by an edge pointing towards the latter. In this work we reverse the edges of this network so that they match the direction of influence in a dynamic model (i.e., if a user trusts another user, the latter has an influence on the opinion of the former). This network was obtained from the Stanford Large Network Dataset Collection <https://snap.stanford.edu/data/>.
 - **arXiv’s High Energy Physics - Theory and High Energy Physics - Phenomenology citation networks [S38, S39]**. Citations between preprints in the e-print repository arXiv for the High Energy Physics - Theory (hep-th) and High Energy Physics - Phenomenology (hep-ph) sections. The citations cover the period from January 1993 to April 2003. Each preprint in the network is denoted by a vertex; a preprint citing another preprint is denoted by a directed edge from the citing preprint to the cited preprint. In this work we reverse the edges of this network so that they match the direction of influence in a dynamic model (i.e., if a preprint is cited by another preprint, the latter had an influence on the former). This network was obtained from the Stanford Large Network Dataset Collection <https://snap.stanford.edu/data/>.
 - **UC Irvine online social network [S40]**. Network of messages among users in an online community for students at University of California, Irvine. Users are denoted by vertices, and a user messaging another user is denoted by an edge pointing towards the latter. This network was obtained from Tore Opsahl’s website <https://toreopsahl.com/datasets/>.
 - **Cellphone communication network [S41]**. Call network of a subset of anonymized cellphone users. Each user is denoted by a vertex, and a call or text message from one user to another is denoted by a directed edge from the sender to the receiver. This network was obtained directly from Yang-Yu Liu.
 - **E-mail communication network [S42]**. Network of e-mails sent among users in a university during a period of 83 days. Each user is denoted by a vertex, and an e-mail sent from one user to another during this period of time is denoted by an edge from the sender to the receiver. This network was obtained directly from Yang-Yu Liu.
 - **Intra-organizational Freeman networks [S43]**. Network of personal relationships among

researchers working on social network analysis at the beginning and at the end of the study. Each researcher is denoted by a vertex, and a personal relationship from a researcher to another is denoted by a directed edge from the former to the latter. In this work we reverse the edges of this network so that they match the direction of influence in a dynamic model (i.e., if a researcher has a personal relationship with another, the latter has an influence on the former). This network was obtained from Tore Opsahl's website <https://toreopsahl.com/datasets/>.

- **Intra-organizational consulting and manufacturing networks [S44]**. Network describing the relationships between employees in a consulting company and in a research team from a manufacturing company. Each employee involved is denoted by a vertex, and the frequency/extent of information or advice an employee obtains from another (as measured by a questionnaire) is denoted by a weighted, directed edge among them that points from the questioned employee. We follow [1] and [6], and use all edges with a nonzero weight to define a unweighted network, which we use for our analysis. We also reverse the edges of this network so that they match the direction of influence in a dynamic model (i.e., if an employee receives advice or information from another, the latter has an influence on the former). This network was obtained from Tore Opsahl's website <https://toreopsahl.com/datasets/>.

III.B. Notes on the ensembles of randomized real networks

We follow [1] and [6], and study the control properties of ensembles of randomized real network using two randomization procedures: full randomization, which turns the network into a directed Erdős-Rényi network with N nodes and M edges [31], and degree-preserving randomization, which keeps the in-degree and out-degree of every node but shuffles its successor and predecessor nodes [32]. Erdős-Rényi randomization is implemented by creating a graph of N nodes, randomly (uniformly) choosing a source and a target of an edge from the set of N nodes, and repeating this for each of the M edges. For the degree-preserving randomization, we start from the original network and choose two edges randomly (uniformly), for which we switch their target nodes if the target and source nodes of both edges are each different (if they are the same, we choose another edge pair). We repeat this step for a transient of $25M$ times, after which we save the obtained network as the first element of the ensemble. We then repeat the target-node-switching step $5M$ times, save the resulting network as the second element of the ensemble, and repeat the target-node-switching step $5M$ times for each consequent ensemble element.

For each real network we used $\Omega = 100$ networks as the ensemble size. For most ensemble properties we used the 100 ensemble networks to estimate the average value and standard deviation of the property, but for some properties this was too computationally expensive for very large networks (e.g. FVS of networks with $> 2.5 \times 10^4$ nodes) or for very dense networks (e.g. cycle numbers of intra-organizational networks). For these properties and networks, we used a smaller ensemble size, as specified below.

- Political blogs. For cycle numbers of length 4, $\Omega = 10$.
- nd.edu. For cycle numbers of length 4, $\Omega = 2$. For N_{FVS} , $\Sigma = 5$ and 1 iteration for GRASP.
- stanford.edu. For cycle numbers of length ≥ 2 , $\Omega = 20$. For N_{FVS} , $\Omega = 5$ and 1 iteration for GRASP.
- Slashdot. For cycle numbers of length ≥ 3 , $\Omega = 20$. For N_{FVS} , $\Omega \geq 40$ and 2 iterations for GRASP.
- Epinions. For N_{FVS} , $\Omega = 50$ and 2 iterations for GRASP.
- arXiv HepTh, HepPh. For cycle numbers of length ≥ 2 , $\Omega = 50$. For N_{FVS} , $\Omega \geq 200$ and ≥ 10 iterations for GRASP.
- UCInonline. For cycle numbers of length 4, $\Omega = 10$.
- Cellphone. For N_{FVS} , $\Omega = 200$ and 50 iterations for GRASP.
- Emails. For cycle numbers of length ≥ 2 , $\Omega = 5$.
- Manufacturing. For cycle numbers of length ≥ 2 , $\Omega = 20$.

IV. Structure-based control of the *Drosophila melanogaster* segment polarity gene regulatory network

We compare the results of the two control methods for the gene regulatory network of the *Drosophila* segment polarity genes, for which several dynamic models exist [34, 35, S45]. The segment polarity genes, especially wingless (*wg*) and engrailed (*en*), are important determinants of embryonic pattern formation and contributors to embryonic development [34]. The wingless mRNA and protein are expressed in the cell that is anterior to the cell that expresses the engrailed and hedgehog (*hh*) mRNA and protein. All models consider a group of four subsequent cells as a repeating unit, and include intra-cellular and inter-cellular interactions.

The continuous model of von Dassow et al. represents each cell as a hexagon with six relevant cell-to-cell boundaries. It includes 136 nodes that represent mRNAs and proteins, among them 4 source nodes and 24 sink nodes, and 488 edges that represent transcriptional regulation, translation, and protein-protein interactions. Fig. 3a in the main text, reproduced here as Fig. S2a, shows the network corresponding to the *wg*-expressing cell (cell 1) and three of its boundaries with the *en*-expressing cell 2. Additional nodes in the network include, *ptc* (patched),

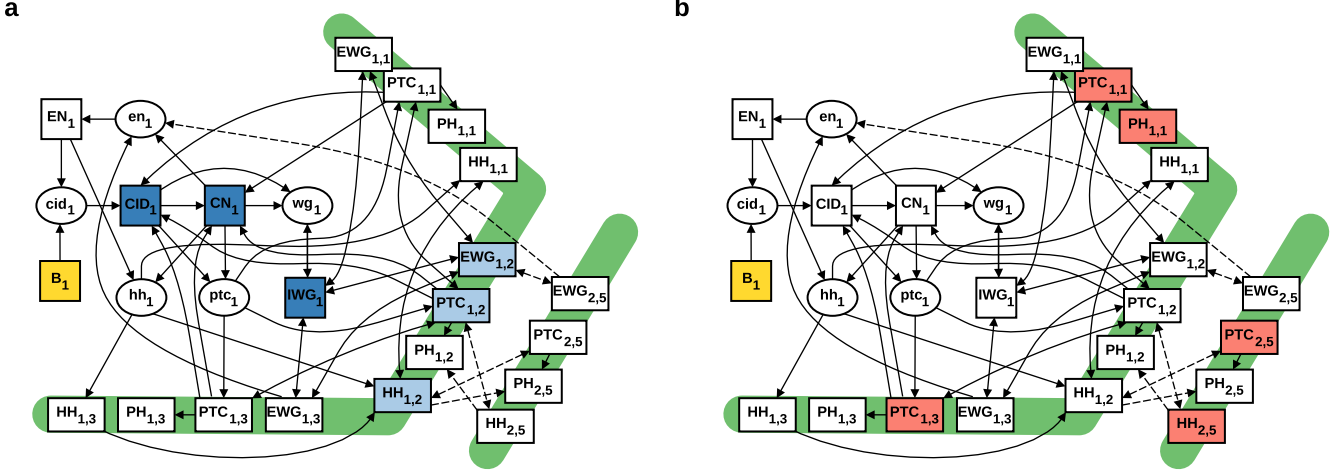


Fig. S2. Control of the von Dassow et al. model of the Drosophila segment polarity network. The figure shows a cell of the four-cell parasegment together with three of its six boundaries (green lines). The complete network contains four cells in a symmetric completion of the figure. Elliptical nodes represent mRNAs and rectangular nodes are proteins. Intracellular interactions are drawn as solid lines and intercellular interactions are dashed. Yellow nodes are source nodes. (a) Blue nodes are FC nodes in every cell. Dark blue nodes are sufficient for attractor control in the considered dynamic models. (b) Red nodes are SC nodes in every cell.

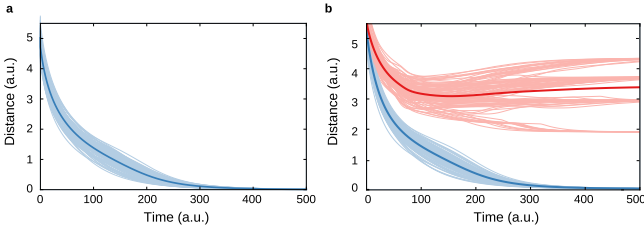


Fig. S3. Effectiveness of the control of the Drosophila segment polarity differential equation model. (a) The thin light blue lines indicate the evolution of the norm of the difference between the desired wild type steady state and the controlled state trajectory using FC (blue symbols on Fig. S2a) for 100 randomly chosen initial conditions. (b) The thin light blue lines are the evolution of the norm of the difference between the wild type steady state and the controlled state trajectory using reduced FC (dark blue symbols on Fig. S2a) for 100 randomly chosen initial conditions. The thin red lines indicate the norm of the difference between the uncontrolled trajectory and the wild type steady state for 100 randomly chosen initial conditions. In all initial conditions the concentration of each quantity is chosen uniformly from the interval $[0, 1]$. The thick blue (red) lines indicate the average of the relevant 100 realizations.

ci (cubitus interruptus), its proteins *CID* and *CN* (repressor fragment of *CID*), *IWG* (intracellular *WG* protein), *EWG* (extracellular *WG* protein), *PH* (complex of patched and hedgehog proteins), and *B*, a constitutive activator of *ci*. For each gene, the mRNA is written in lower case and the protein(s) are written in upper case. The nodes are characterized by continuous concentrations, whose rate of change is described by ordinary differential equations (ODE) involving Hill functions for gene regulation and mass action kinetics for protein-level processes, and using 48 kinetic parameters [S46, S47]. von Dassow et al. have shown that the model can re-

produce the essential feature of the wild type steady state: *wg/WG* are expressed anterior to the parasegment boundary (cell 1) and *en/EN/hh/HH* are expressed posterior to the parasegment boundary (cell 2) as shown in Fig. 3. The initial condition that yields this steady state for the most parameter sets, the so-called “crisp” initial condition, *wg/IWG* in the first cell is at maximal concentration (1), *en/EN* in the second cell has concentration 1, the source nodes *B* are fixed at 0.4 in each cell and all the other nodes have zero concentration.

Wild type steady state of the von Dassow et al. model for the second parameter set provided by the *Ingenue* program [S46, S48], using normalized concentration variables

$$\begin{aligned}
 c(en_2) &= c(EN_2) = 0.986, \\
 c(wg_1) &= 0.857, \\
 c(IWG_1) &= 0.006, \\
 c(EWG_{0,0}) &= c(EWG_{0,3-5}) = 0.005, \\
 c(EWG_{0,1}) &= c(EWG_{0,2}) = 0.011, \\
 c(EWG_{1,0}) &= c(EWG_{1,3}) = 0.269, \\
 c(EWG_{1,1-2}) &= c(EWG_{1,4-5}) = 0.264, \\
 c(EWG_{2,0-3}) &= 0.005, \\
 c(EWG_{2,4}) &= c(EWG_{2,5}) = 0.011, \\
 c(ptc_0) &= c(ptc_1) = c(ptc_3) = 0.995, \\
 c(ptc_2) &= 0.001, \\
 c(PTC_{0,*}) &= c(PTC_{1,*}) = c(PTC_{3,*}) = 0.166, \\
 c(ci_0) &= c(ci_1) = c(ci_3) = 0.868, \\
 c(ci_2) &= 0.007, \\
 c(CI_0) &= c(CI_1) = c(CI_3) = 0.057, \\
 c(CI_2) &= 0.005,
 \end{aligned}$$

$$\begin{aligned}
c(CN_0) &= c(CN_1) = c(CN_3) = 0.42, \\
c(CN_2) &= 0.001, \\
c(hh_2) &= 1, \\
c(HH_{2,0}) &= c(HH_{2,3}) = 0.072, \\
c(PH_{1,1-2}) &= c(PH_{3,4-5}) = 0.001,
\end{aligned}$$

where $i, *$ represents all sides of the i th cell. The concentration of the other nodes is smaller than 10^{-5} .

Another initial condition considered here is a nearly-null initial condition, wherein intra-cellular nodes have a concentration of 0.05 in the first and third cell and 0.15 in the second and fourth (zeroth) cell; membrane-localized nodes have concentration of 0.15 for even-numbered sides and 0.05 for odd-numbered sides in every cell. This initial condition yields an unpatterned steady state for the majority of parameter sets.

Unpatterned steady state of the von Dassow et al. model, for the second parameter set provided by the *Ingeneue* program [S46, S48], using normalized concentrations:

$$\begin{aligned}
c(wg_*) &= 0.857, \\
c(IWG_*) &= 0.007 \\
c(EWG_{*,*}) &= 0.28, \\
c(ptc_*) &= 0.996, \\
c(PTC_{*,*}) &= 0.166, \\
c(ci_*) &= 0.868, \\
c(CI_*) &= 0.057, \\
c(CN_*) &= 0.42,
\end{aligned}$$

where $*$ represents for all cells, and $*, *$ represents for all sides in all cells. The concentration of the other nodes is smaller than 10^{-5} .

The differential equation system is solved using a custom code in Python and the `odeint` function with default parameter setting. We used the differential equations given in the appendix of [S47]. *Ingeneue* can be found at <http://rusty.fhl.washington.edu/ingeneue/papers/papers.html>.

The Boolean model implements a few modifications in the network topology compared with the ODE network model, and considers only two cell-to-cell boundaries instead of six. There are 56 nodes and 144 edges in the network as shown in Fig. 3b. One difference compared with the von Dassow et al. model is the existence of three cubitus interruptus proteins: the main protein *CI*, and two derivatives with opposite function: *CIA*, which is a transcriptional activator, and *CIR*, a transcriptional repressor. There are four source nodes, representing the sloppy paired protein (*SLP*), which is known to have a sustained expression in two adjacent cells (cells 0 and 1 if the *wg*-expressing cell is considered cell 1) and is absent from the other two. There are ten steady states for this Boolean network model when considering the biologically relevant pattern of the source node states. Starting from the biologically known wild type initial condition, which

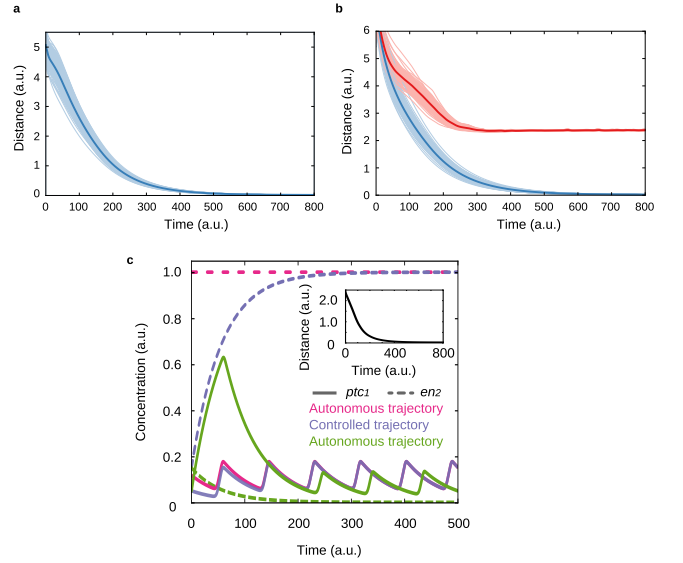


Fig. S4. Control of the Drosophila segment polarity gene differential equation model for a different parameter set than that used to generate Fig. 3. (a) The thin light blue lines show the evolution of the norm of the difference between the wild type attractor and the controlled state trajectory using FC for 100 randomly chosen initial conditions. (b) The thin light blue lines are the evolution of the norm of the difference between the wild type attractor and the controlled state trajectory using reduced feedback FC for 100 randomly chosen initial conditions. The thin red lines are the evolution of the norm of the difference between the wild type attractor and uncontrolled trajectory using reduced FC for 100 randomly chosen initial conditions. In all initial conditions the concentration of each quantity is chosen uniformly from the interval $[0,1]$. The thick blue(red) line is the average of the 100 realizations. (c) The concentration of *ptc* in the first cell (solid lines) and *en* in the second cell (dashed lines) with respect to time. Pink lines and green lines represent autonomous trajectories that start from different initial conditions (a wild type initial condition and a nearly null, respectively) and converge to different attractors (the wild type limit cycle and an unpatterned limit cycle, respectively). Blue lines represent the case when the system starts from the nearly null initial condition, and after applying FC, evolves into the wild type limit cycle. Inset: evolution of the norm of the difference between the desired attractor and the controlled state trajectory using FC.

consists of the expression (ON state) of *SLP*₀, *SLP*₁, *wg*₁, *en*₂, *hh*₂, *ci*₀, *ci*₁, *ci*₃, *ptc*₀, *ptc*₁, *ptc*₃, the model converges into the biologically known wild type steady state illustrated on Fig. 3c.

Specifically, the wild type steady state of the Albert & Othmer model consists of the expression of

$$\begin{aligned}
&SLP_0, SLP_1, wg_1, WG_1, en_2, EN_2, hh_2, HH_2, \\
&ci_0, ci_1, ci_3, CI_0, CI_1, CI_3, CIA_1, CIA_3, CIR_0, \\
&ptc_1, ptc_3, PTC_0, PTC_1, PTC_3, PH_1, PH_3.
\end{aligned}$$

Analytical solution reported in [S47] indicated that the states of the *wg* and *PTC* nodes, each of which has a positive auto-regulatory loop, determine the steady state for the given source node (*SLP*) configuration [35]. For example, any initial condition with no *wg* expression leads to an unpatterned steady state wherein *ptc*, *ci*, *CI* and

CIR are expressed in each cell, and the rest of the nodes are not expressed in any cell.

IV.A. Structure-based control of the von Dassow et al. differential equation model

The FC method predicts that one needs to control $N_{FC} = 52$ nodes (4 source nodes and 48 additional nodes) to lead any initial condition to converge to any original attractor of the model. There are multiple control sets with $N_{FC} = 52$; one of them consists of B (source node), CI , CN , IWG , EWG on every other side, HH on every other side, PTC on every other side in all four cells (shown in Fig. S2a). We perform simulations using two benchmark parameter sets to test this prediction. We use the second parameter set provided by the Ingenu program to test the system's convergence to a steady state [S46, S48]. The ODE system has at least two steady states with this parameter set. A nearly null initial condition leads to the unpatterned state (illustrated by the green lines in Fig. 3d in the main text). The crisp initial condition leads to the wild type pattern (see pink lines in Fig. 3d), which we choose as the desired steady state. If we start from the nearly null initial condition and maintain the concentrations of the nodes in the FC node set in the values they would have in the desired steady state, the system evolves into the desired steady state (see blue lines and inset of Fig. 3d). We obtained the same success of FC control when starting from 100 different random initial conditions (shown in Fig. S3a). We also obtained the same success using a reduced FC set (blue lines in Fig. S3b), which consists of B , CID , CN , IWG in every cell. In contrast, in the absence of control none of the trajectories converge to the wild type steady state (red lines in Fig. S3b).

We also numerically verified, using a different benchmark parameter set, namely the first parameter set provided by the Ingenu program, that FC control can also successfully drive any state to a limit cycle attractor (see Fig. S4a). This limit cycle attractor has the same expression pattern of en , wg and hh as the wild type steady state, thus we refer to it as the wild type limit cycle (illustrated in Fig. S4c). We also obtained the same success of driving any state to a limit cycle attractor using the same reduced Feedback vertex control shown in Fig. S4b.

SC control indicates multiple control sets with $N_{SC} = 24$ nodes. One possible combination is B_* , $PTC_{*,1}$, $PTC_{*,3}$, $PTC_{*,5}$, $HH_{*,5}$, $PH_{*,1}$, where $*$ represents all cells (shown in Fig. S2b). Though SC predicts that less nodes need to be controlled, applying it requires a potentially complicated time-varying driver signal, which would need to be determined for each initial condition using, for example, minimum-energy control or optimal

control [9, 18].

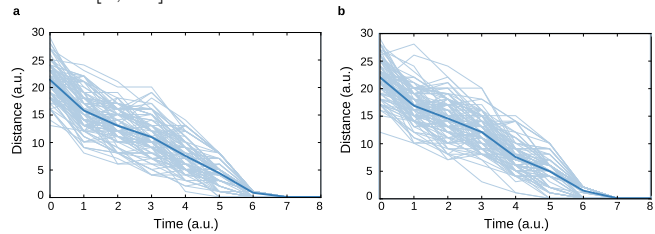


Fig. S5. Control of the Boolean model of the Drosophila segment polarity genes. The light blue thin lines show the evolution of the norm of the difference between the wild type steady state and the controlled state trajectory using feedback vertex set control (FC) for 100 randomly chosen initial conditions, in which the concentration of each quantity is chosen between ON and OFF with equal odds. The thick blue line is the average of the 100 realizations. (a) Control using the feedback vertex set (b) Control using the reduced feedback vertex set.

IV.B. Structure-based control of the Albert & Othmer Boolean model

The FC method predicts that $N_{FC} = 14$ nodes need to be controlled, including the 4 source nodes (SLP), the 8 self-sustaining nodes (all wg and PTC), and 2 additional nodes (with one possibility being CIR_1 and CIR_3). Since the FC set contains all wg and PTC nodes, which were shown to determine the steady states under the indicated source node states, we can conclude that controlling the nodes in the FC set is enough to drive any initial condition to the desired steady state in the Albert & Othmer model. The simulation result is consistent with the theoretical result, as shown in Fig. 3e. The wild type initial condition leads to the wild type steady state (pink lines). The null initial condition used in the Boolean model is that all the nodes are in the OFF state; the resulting steady state is the unpatterned steady state (green lines). The controlled trajectory with FC is shown in blue lines. We obtained the same success of FC control when starting from 100 different random initial conditions, as shown in Fig. S5a. Moreover, the 12 nodes consisting of SLP , wg and PTC in each cell (which we refer to as the reduced FC set) are enough to drive all the random initial conditions to the desired steady state in this particular model, as shown in Fig. S5b.

SC control predicts that we only need to control the four source nodes as the network can be covered by four branches and one loop. For a simplified, single-cell version of the Albert & Othmer model, Gates and Rocha showed that the SC node set is sufficient for attractor control, but does not fully control this system [S49]. Thus, a control method such as [S50, S51] seems to be required for correctly predicting full control node sets in Boolean models.